Helsinki University of Technology
Optics and Molecular Materials
Espoo 2001

FLOW AND CONDUCTIVITY PROPERTIES OF COMB-SHAPED SELF-ORGANIZED SUPRAMOLECULES

Riikka Mäki-Ontto *nee* Mäkinen

Dissertation for the degree of Doctor of Philosophy to be presented with due permission for public examination and debate in Auditorium F1 at Helsinki University of Technology (Espoo, Finland) on 23rd of November, 2001, at 12 o'clock noon.

Helsinki University of Technology
Department of Engineering Physics and Mathematics
Optics and Molecular Materials

Teknillinen korkeakoulu
Teknillisen fysiikan ja matematiikan osasto
Optiikka ja molekyylimateriaalit

Distribution:
Helsinki University of Technology
Optics and Molecular Materials
P.O. Box 2200
FIN-02015 HUT
Tel. +358-9-451 3153
Fax. +358-9-451 3164
Email: riikka@focus.hut.fi

ISBN 951-22-5733-5

Otamedia Oy
Espoo 2001

Preface

This work has been carried out at the Department of Engineering Physics and Mathematics in Helsinki University of Technology under supervision of Professor Olli Ikkala and visiting Professor Gerrit ten Brinke from University of Groningen.

First of all, I would like to thank them for all the supervision and enthusiasm.

I would like to thank my collaborator Dr. Karin De Moel for the valuable and significant teamwork during my measurement trips to Mainz and Groningen. During the research for this Thesis she has become more a friend than a collaborator.

I would like to thank Professor Manfred Stamm for collaboration at Max Planck Institute for Polymer Research in Mainz and at Institute for Polymer Research in Dresden Germany. I would like to thank Walter De Odorico for his help with SAXS and for nice atmosphere while measuring in Mainz.

I wish to thank also several coworkers: Doc. Ritva Serimaa and Dr. Mika Torkkeli at University of Helsinki, Dr. Evgeny Polushkin and Gert Alberda van Ekenstein at University of Groningen. I would like to express my warmest thanks to Lic.Sc. Tapio Mäkelä at VTT Microelectronics for his advises in conductivity measurements. I would like to thank the former and present members of our research group, Dr. Janne Ruokolainen, M.Sc. Juha Tanner, Dr. Mika Saariaho, M.Sc. Sami Valkama, M.Sc. Matti Knaapila, M.Sc. Harri Kosonen, M.Sc. Juha Hartikainen, M.Sc. Olli Lehtonen, M.Sc. Panu Hiekkataipale, Mr. Teemu Ruotsalainen and last but definitely not least M.Sc. Mari Tiitu for a nice working environment.

I am grateful to National Graduate School of Molecular Nanotechnology and Prof. Helge Lemmetyinen as well as Technology Development Center of Finland (TEKES) for funding my doctoral studies. Personal scholarships from the Foundation of Technology are gratefully acknowledged.

Finally I wish to thank my mother for all the support over the years and my dear husband Petri for all the patience and encouragement during this work. I would also like to thank Ketty and Kaija for being so excellent friends.

Espoo, November 2001

Riikka Mäki-Ontto *nee* Mäkinen

List of Publications

I. J. Ruokolainen, **R. Mäkinen**, M. Torkkeli, R. Serimaa, T. Mäkelä, G. ten Brinke, O. T. Ikkala*, Switching Supramolecular Polymeric Materials with Multiple Length Scales,* Science **1998**, 280, 557-560.

II. O. Ikkala, J. Ruokolainen, **R. Mäkinen**, M. Torkkeli, R. Serimaa, T. Mäkelä, and G. ten Brinke, *Electrical Switching Based On Dimensionality Transitions in Nanostructured Polymers*, Synthetic Metals **1999,** 102, 1498-1501.

III. **R. Mäkinen**, J. Ruokolainen, O. Ikkala, K. de Moel, G. ten Brinke, W. De Odorico, and M. Stamm, *Orientation of Supramolecular Self-Organized Polymeric Nanostructures by Oscillatory Shear Flow*, Macromolecules, **2000**, 33, 3441-3446.

IV. K. de Moel, **R. Mäki-Ontto,** M. Stamm, G. ten Brinke, and O. Ikkala, *Oscillatory Shear Flow Induced Alignment of Lamellar Melts of Hydrogen Bonded Comb Copolymer Supramolecules,* Macromolecules **2001**, 34, 2892-2900.

V. **R. Mäki-Ontto**, K. de Moel, E. Polushkin, G. Alberda van Ekenstein, G. ten Brinke, and O. Ikkala, *"Tridirectional protonic conductivity in soft materials"*, Report TKK-F-A809 **2001**, submitted to Advanced Materials

VI. **R. Mäki-Ontto,** K. de Moel, W. de Odorico, J. Ruokolainen, M. Stamm, G. ten Brinke, and O. Ikkala *"Hairy Tubes": Mesoporous Materials Containing Hollow Self-Organized Cylinders with Polymer Brushes at the Walls,* Advanced Materials, **2001**, 13, 117-121.

Author's Contribution

The author has taken part in all stages of the design and realization of the experimental work presented in this Thesis. In particular the author is responsible for all the AC conductivity measurements. She has also done a great part of the rheological measurements and small angle X-ray studies (SAXS) measurements in Articles III, IV and VI.

The SAXS measurements in Article I and II were performed in University of Helsinki in collaboration with Doc. Ritva Serimaa and Dr. Mika Torkkeli. The SAXS and rheological measurements in Articles III and part of the measurements in Article IV were performed by the author and Dr. Karin de Moel at Max-Planck Institute for Polymer Research in Mainz, Germany in collaboration with the group of Professor Manfred Stamm. The rest of the SAXS measurements in Article IV were done mainly by the author at the University of Groningen, the Netherlands. The SAXS measurements in Article VI were performed by the author at the University of Groningen, the Netherlands. The rheological measurements in Article VI were performed by the author at the Institute for Polymer Research in Dresden, Germany in collaboration with the group of Professor Manfred Stam. The conductivity measurements in Articles I, II, and V were done by the author at VTT Microelectronics in collaboration with Lic.Tech. Tapio Mäkelä.

The author has actively participated in reporting the research in Articles I-VI. Articles III, V and VI were primarily written by author. Author has presented the results covered in this Thesis at several international conferences.

Contents

1. Introduction

1.1. Self-organized materials

Self-organization of polymers to achieve nanoscale structures has been widely studied. Examples of such systems are liquid crystalline polymers (1), block copolymers (2) and polymer-amphiphile complexes (see for example (3-7)). They form nanostructures due to repulsive and attractive forces within the system. [1]

Probably the most common self-organized polymers are diblock copolymers, which consist of two polymer blocks A and B, which are covalently bonded to each other. Due to repulsive forces between them, the material microphase separates to form nanostructures such as spherical, cylindrical and lamellar structures (2).

A more complicated example is polymer-amphiphile complex where the amphiphiles are bonded to the polymer backbone via physical bonding such as ionic, coordination or hydrogen bonding (3-5, 8-11). Due to the physical nature of this bonding, there must be equilibrium between the attraction i.e. the strength of the polymer-amphiphile interaction and repulsion between the polar polymer backbone and nonpolar alkyl tail. If either the repulsion or attraction is too weak, the self-organized structure cannot be formed.

In this work we have used two types of materials. The first one is a polymer-amphiphile complex which consists of a polymer backbone with amphiphiles attached via hydrogen bonging or ionic bonding to each repeat unit of the backbone resulting in comb-shaped supramolecules which self-organize typically into lamellar structures (9, 12, 13).

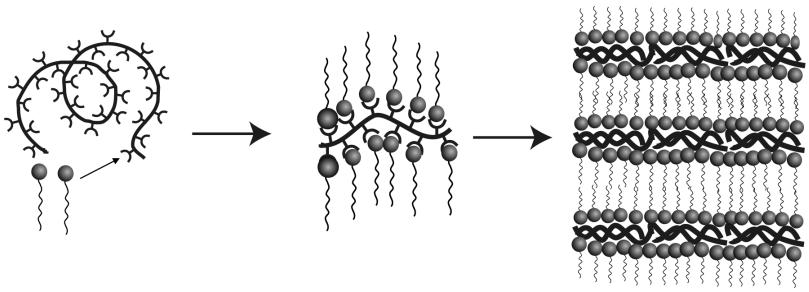

Figure 1. Scheme of a self–organized polymer-amphiphile complex. The polymer has recognition sites, where the amphiphiles are attached via e.g. hydrogen bonding to form comb-shaped supramolecules. Due to repulsive forces between polymer backbone and tails of amphiphiles the self-organized structure is formed.

The second type of structure is formed when a block copolymer structure and polymer-amphiphile structure are combined. In this case the block copolymer is chosen so that one block B can form a polymer amphiphile complex whereas block A cannot, which leads to a hierarchical self-organized structure. The larger structure has the periodicity of 200-1000 Å and the smaller structure 20-50 Å (Figure 2). Depending of the block lengths, the resulting structure can be lamellar-*within*-lamellar, lamellar-*within*-cylinder, lamellar-*within*-spheres etc. (11, 14, 15).

[1] Self-organization within the present context means the same as microphase separation

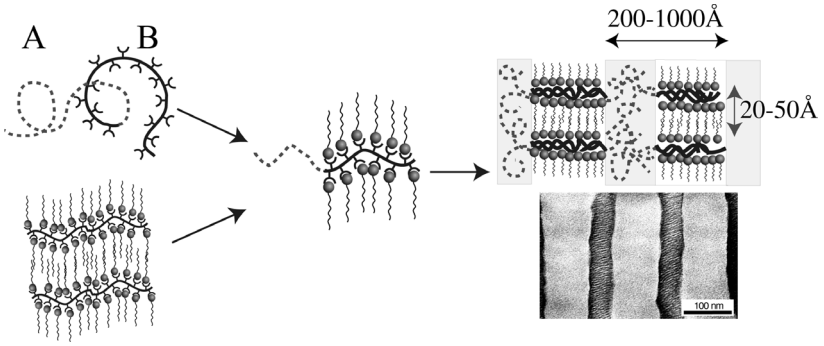

Figure 2. A scheme for hierarchical nanostructures. A block copolymer structure is combined with a polymer –amphiphile structure resulting in nanoscale structures with the larger structure having a periodicity of 200-1000 Å and the inner structure of 20-50 Å. TEM picture by J. Ruokolainen.

1.2. Oscillatory shear flow

An aim has been to combine self-organization and functionalities in order to achieve new kinds of polymeric materials. A problem has been that self-organization does not, as such, have macroscopic order (for example TEM picture in Figure 28) and therefore the local structures need to be aligned (Figure 3). Several methods have been proposed and used to achieve “single crystal -like” structures in these materials. External fields such as electric (16-19), magnetic (20) and in particular flow fields have been studied.

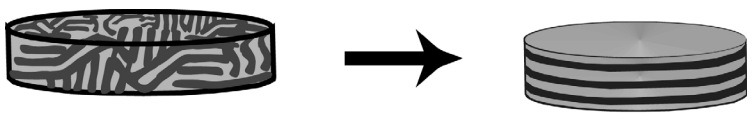

Figure 3. Schematic picture of a self-organized material before and after alignment

Studies have been done for block copolymers poly(ethylene-propylene)-poly(ethylethylene), PEP-PEE and polystyrene-polyisoprene, PS-PI. Alignment diagrams have been presented for both materials (Figure 4) where the final alignment depends on the temperature and frequency used. There are four different regimes with different final alignments and aligning mechanisms (21-23). In the low frequency regime the final alignment tends to be parallel to the shearing plates (24-26) in some systems e.g. in PEP-PEE, whereas for some systems e.g. PS-PI regime I is not observed (21, 27, 28). The parallel alignment in regime I is due to such a low shear frequency that the polymer chains and lamellae are fully relaxed and shearing only deforms the domains and disturbs the defects between them (23). In the intermediate frequency regime (II) the final alignment is perpendicular. This regime is found close to the order-disorder transition temperatures of the structure. It has been suggested that the perpendicular orientation in the intermediate frequency regime is due to destruction and reorganization of the lamellar structure (22-25). In the regimes III and IV the final alignment is parallel but the routes are different. In the regime III there are first both perpendicular and parallel alignments present but the strength of mechanism towards the parallel alignment increases

more rapidly with strain amplitude resulting in the parallel alignment (29, 30). In the regime IV the resulting parallel alignment grows from the biaxial parallel transverse orientation. It was suggested that this is due to an entanglement effect and elongation of chains (31).

Between regimes I and II, as well as between II and III there are characteristic frequencies, ω_c and ω_d. ω_c describes the frequency below which the dynamical properties are controlled by the microdomain structure and the time-temperature superposition principle may not apply (24). The other characteristic frequency ω_d has been less studied (22, 24), but it can be associated with the crossover between regimes I and II (22).

Various methods have been used in this field: light scattering together with ex-situ transmission electron microscopy, TEM and (21, 23, 26, 28-30, 32) small angle X-ray scattering, SAXS (31, 33-37) as well as small angle neutron scattering (SANS) in-situ and ex-situ (24). An excellent review is presented by Chen and Kornfield with more details (23).

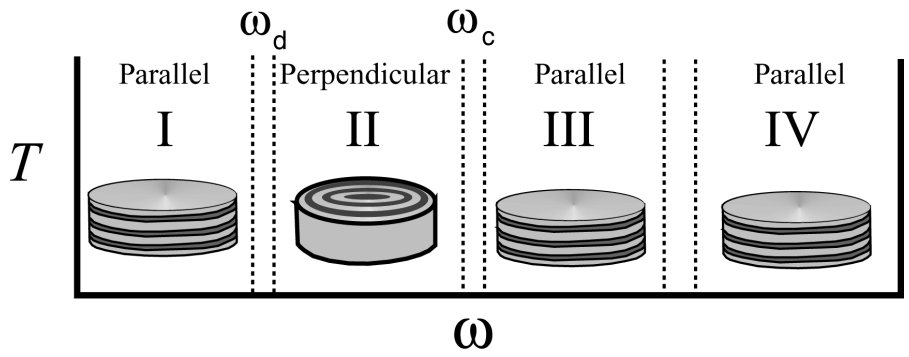

Figure 4. A scheme for different frequency regimes found for PEP-PEE and PS-PI. Regime I is not observed for PS-PI.

Liquid crystalline polymers under shear flow have been widely studied (e.g. ref. (1)). However, there are only few studies on the flow of side chain liquid crystalline polymers (38-42), which are more related to the present material. The disadvantage in orienting side chain liquid crystalline polymers using an oscillatory shear flow seems to be the quick relaxation of the material. As soon as the shear flow is removed the material tends to unalign again (40).

1.3. Protonically conducting polymers

Ionically conducting polymeric materials have been under interest because of their potential for various electrochemical applications such as high energy density batteries and polymer fuel cells (43). Poly(ethylene oxide), PEO, and poly(propylene oxide), PPO, based electrolytes are widely studied because they form complexes with alkali metal (such as Lithium) salts (44-46). Protonically conducting membranes of polymeric perfluorinated ionomers (such as Nafion and Dow) are one of the best-known fuel cell membrane material with high chemical stability. The main disadvantages in these materials are their high price and the production process, which includes strongly toxic and environmentally unfriendly intermediates. A recent review on fuel cell membranes is in ref. (47). Also several

other proton-conducting materials have been studied especially acid-base complexes e.g. ref. (48-51).

Polymer electrolytes characteristically show improved conductivity at elevated temperatures. In most cases the conductivity obeys either Arrhenius law or Vogel-Tamman-Fulcher (VTF) equation.

Usually at low temperatures such as below and close to the glass transition temperature, T_g, the conductivity obeys the Arrhenius law

$$\sigma = \frac{A}{T}\exp(-E_a / kT),$$

where E_a is the activation energy. This formula has been derived in e.g. ref. (52) based on the self-diffusion in a single crystal.

Above T_g and for materials, which are amorphous throughout the available temperature range, the material usually follows the VTF formula

$$\sigma = \frac{A}{\sqrt{T}}\exp(-B/(T - T_0)),$$

where B is a pseudo activation energy related to the segmental motions of the polymer, A is a constant and T_0 is typically 30-50°C below T_g and is called equilibrium glass transition temperature (53, 54). More details on VTF equation are found in ref.(52).

Three most typical forms of conductivity behavior of polymer electrolytes are (55): a) material with VTF behavior throughout the available temperature range, b) Arrhenius behavior at low temperatures and VTF at high temperatures and c) Arrhenius type of behavior throughout the whole temperature range with a clear decrease of the activation energy around the T_g. A more detailed treatment of the different conductivity mechanisms in polymer electrolytes can be found in ref.(55).

1.4. An outline of this Thesis

In this Thesis we have studied self-organization of comb-shaped supramolecules i.e. polymer-amphiphile complexes (Figure 1) and hierarchically self-organized supramolecules i.e. block copolymer amphiphile complexes (Figure 2) in an oscillatory shear flow. We have also studied the conductivity of such structures. We start with the Articles I-II, which describe self-organized hierarchical polymeric materials with peculiar conductivity behavior allowing temperature control of conductivity. However, this structure is not macroscopically aligned and therefore the conductivity is isotropic throughout the sample. In order to macroscopically align this material and study the conductivity through different nanoscale layers we investigate these hierarchical structures under the shear flow (Articles III-V). In Article V we have combined the knowledge in order to achieve anisotropic conductor to show tridirectional conductivity i.e. material, which has different conductivity values in the three spatial directions. We also show that this has a connection to the hopping conductivity in the material. This covers this work as reported in Articles I-V. We have also used the related principles to achieve mesoporous materials, which are described in Article VI.

Chapter 2 represents the materials used. In Chapter 3 we briefly describe the two-dimensional SAXS setup and the principle of the rheological measurements. The rest of Chapter 3 concentrates on the AC-impedance method and the experimental setup used.

The main results of Articles I-V are presented in Chapter 4. The results are presented with a short overview of related work done in the field. Chapter 5 shows an approach to prepare mesoporous materials based on the hierarchical self-organization of supramolecular materials. Conclusions and some future prospects are presented in Chapter 6.

2. Materials

The abbreviations of the materials used are listed in Table I

Table I. Abbreviations of materials used

Materials	**Abbreviation**
polystyrene	PS
poly(4-vinylpyridine)	P4VP
n-pentadecylphenol	PDP
methanesulphonic acid	MSA
p-toluenesulphonic acid	TSA

The complexes were prepared by dissolving all the components into common solvent followed by its evaporation. More details are presented in Articles I-VI.

The materials used in this Thesis can be divided in two different ways. The first division is based on the structure. The materials with only one self-organized supramolecular structure are in one group and hierarchical supramolecular materials in another (Table II). The second division is based on the conductivity. One group is formed by the protonically conducting structures and the other group by the nonconducting structures (Table II).

Table II. Nomenclature for complexes, the conducting materials are marked as*.

Name		**Complex**
Self-organized supramolecule	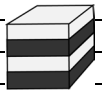	$P4VP(MSA)_{1.0}PDP_{1.0}$ *
		$P4VP(TSA)_{1.0}PDP_{1.0}$ *
		$P4VP(PDP)_{1.0}$
Hierarchical self-organized	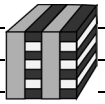	PS-*block*-$P4VP(MSA)_{1.0}PDP_{1.0}$ *
supramolecule		PS-*block*-$P4VP(TSA)_{1.0}PDP_{1.0}$ *
		PS-*block*-$P4VP(PDP)_{1.0}$

The chemical formulas are presented in Figure 5 in the same order than they are introduced in Chapter 4.

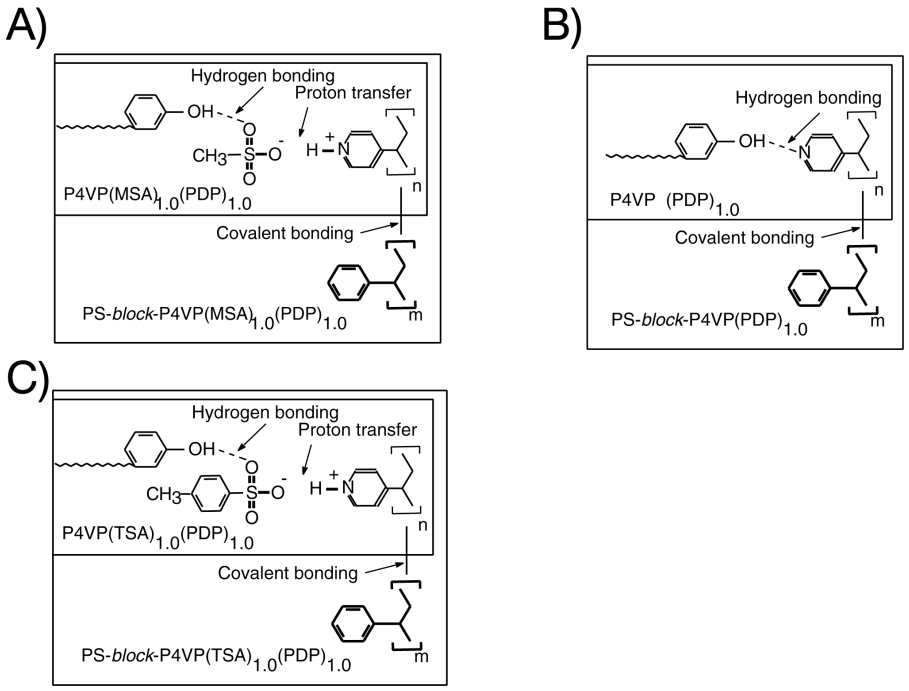

Figure 5. Chemical formulas of materials studied in Articles I-VI.

3. Experimental methods

In this section we first briefly describe the Small-Angle X-ray Scattering (SAXS) and the rheological experiments. The rest of this section concentrates on the details of the AC-impedance method, and the experimental setup used.

3.1. In-situ and ex-situ SAXS

The Small Angle X-ray Scattering (SAXS) measurements were performed at different laboratories. The measurements in Articles I-II were done at the University of Helsinki in collaboration with Docent Ritva Serimaa, whereas the measurements in Articles III and IV were done at Max-Planck Institute for Polymer Research in collaboration with the group of Professor Manfred Stamm (Mainz Germany) and at University of Groningen, in collaboration with the group of Professor Gerrit ten Brinke (the Netherlands). Measurements in Articles V and VI were at the University of Groningen. The details of the setup at Helsinki are presented in Articles I and II.

At Max Planck Institute for Polymer Research the changes of structure was measured *in-situ* under the shear flow. The schematic of the setup is shown in Figure 6. The rheometer was placed in such a way that the beam penetrated the sample at approximately 1 mm from the rim. The direction of the beam was therefore the same as the flow direction, i.e. tangential. As a result, we were able to determine the changes of the structure during shearing the sample. More details are presented in Articles III and IV.

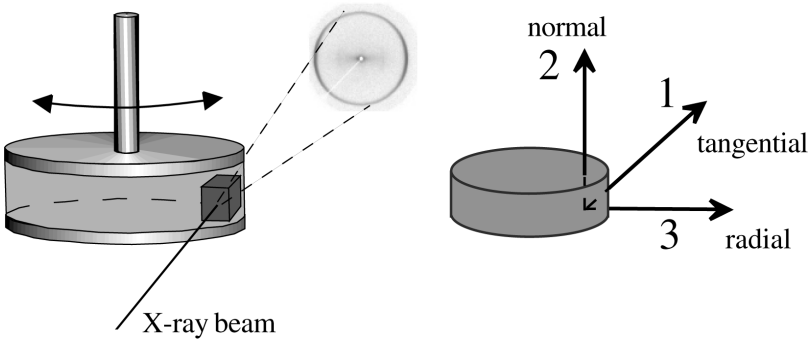

Figure 6. Schematics of in-situ SAXS measurement. The X-ray beam penetrates the sample approximately 1 mm from the outer rim. The changes of the x-ray pattern are monitored. The figure in the right shows the directions used throughout this Thesis. 1 is the flow direction (tangential), 2 is the shear gradient direction (normal), and 3 is neutral direction (radial) pointing from the center of the tablet to the rim.

After shearing the sample was cooled down and removed in order to measure the SAXS patterns in the three directions. In Figure 7 there is an example of such measurement with P4VP(TSA)$_{1.0}$(PDP)$_{1.0}$, showing a parallel orientation. In Groningen it was not possible to make simultaneous SAXS and rheology and therefore the measurements were done only *ex-situ*. More details of the measurement setup at University of Groningen are presented in Articles IV-VI.

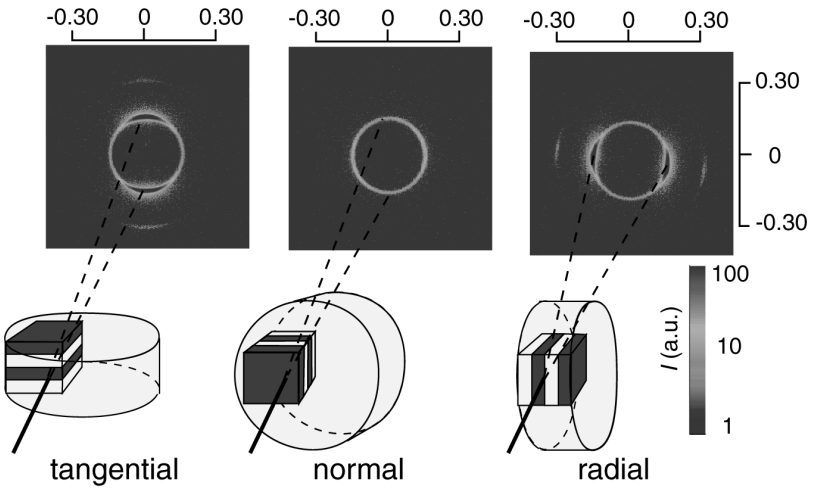

Figure 7. Schematics of ex-situ SAXS experiment. X-ray patterns are taken in three directions in order to determine the final structure. The units of the scattering vector q are in 1/Å.

3.2. Rheological measurements

The rheological measurements were performed with different setups of dynamic rheometer with plate-plate and cone-plate geometries using various temperature profiles (Articles III-VI for details). Figure 8 represents the schematics of the oscillatory shear flow. The material is placed between two plates and heated to the desired temperature. The other plate oscillates with a selected frequency and strain amplitude resulting increase of macroscopic alignment. Depending on the temperature, oscillation frequency, and strain amplitude, the resulting alignment in the case of lamellar structure may be parallel (i.e. the layer normals along the shear gradient direction), perpendicular (the layer normals along the vorticity direction) or transverse (the layer normal along the flow direction) or combinations of them.

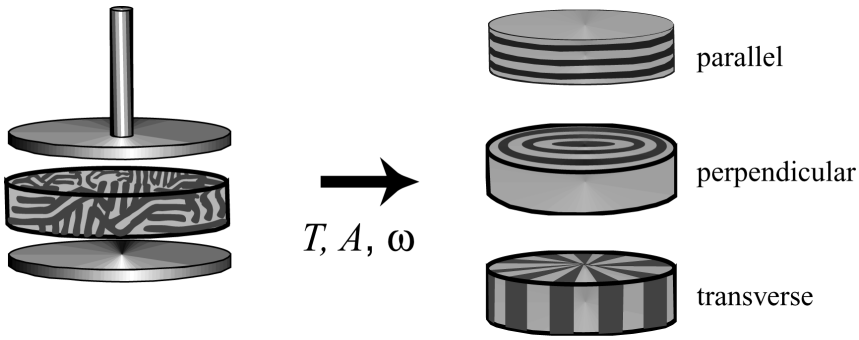

Figure 8. Schematics of the setup using parallel plate geometry and the three orientations observed in the case of block copolymers. Depending on the temperature, frequency and strain used, the final alignment can be parallel, perpendicular, or transverse.

3.3. On the protonic conductivity measurements

Various methods have been used to measure conductivity properties (see e.g. ref. (43, 56-59). In electronic conductors most common method is four-point measurement with a direct current (DC). Its advantages are that the measurement wires and the contact resistance do not play a role and the measurement system is simple. However, it ideally requires samples that are long compared to their cross section.

Another method is an alternating current (AC) impedance measurement. It is more complicated and needs some knowledge of the theory. On the other hand the AC-impedance method can be applied also to ionically conducting materials giving more information about the nature of the conductivity. In this work there was also another advantage in using the AC-impedance method: because the samples were aligned we wanted to measure the conductivity in specific directions. Due to relatively small and nearly rectangular (1 mm x 1 mm x 2mm) samples, the most convenient way to measure the conductivity was to place the sample between two electrodes. The disadvantage in the AC-impedance system is due to the errors caused by the contact resistance between the platinum electrodes and the sample. However, when relatively high frequencies are used (such as 1 kHz) the effect of the contact resistance is negligible as will be discussed shortly. Another disadvantage is due to two-probe measurement setup where the measurement wires give their part into the measured resistance. However, the conductivity levels of all the materials discussed in this Thesis are low compared to the conductivity of the wires and therefore the error was found to be negligible.

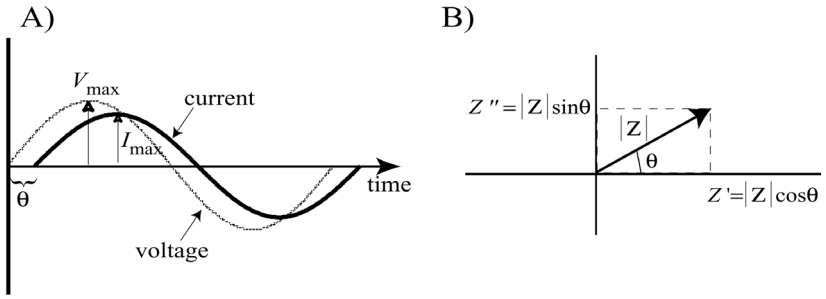

Figure 9. A) In the AC-impedance method a sinusoidal voltage is applied and the current passing through the sample is measured. B) Impedance spectrum presented in complex plane. *Z'* and *Z''* represents the real and imaginary components of impedance *Z**.

In AC-conductivity measurements a sinusoidal voltage is applied and the current passing through the sample is measured. As a result impedance Z* [2] is a

[2]Some authors have used different formalism when presenting the AC impedance results based on admittance (*Y**), permittivity (ε*) and electric modulus (*M**), which all are related to *Z** with the following formulas

$$Y^* = \frac{1}{Z^*} = j\omega C_0 \varepsilon^*$$

$$M^* = \frac{1}{\varepsilon^*} = j\omega C_0 Z^*,$$

where the angular frequency $\omega = 2\pi f$ and C_0 is the vacuum capacitance of the cell

complex presentation of the ratio of voltage and current maxima, $|Z| = V_{max} / I_{max}$ and phase angle θ, the phase difference between voltage and current (Figure 9 a). The result may also be represented in a complex plane with $Z^* = Z' - jZ''$ (Figure 9 b).

In the AC impedance measurement the impedance is measured as a function of frequency. The impedance spectrum is typically presented in the Z', Z''-complex plane. It is possible to construct an equivalent electrical circuit consisting of resistors and capacitors, which have the same frequency response as the measured material (for example Figure 10). These equivalent circuits give us further information on the conduction processes in the material.

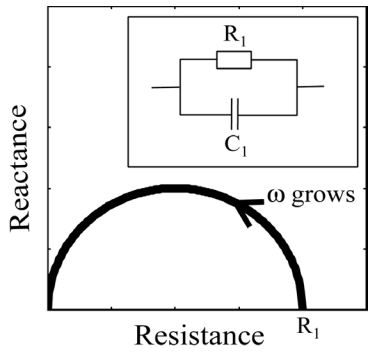

Figure 10. The Z', Z'' or resistance-reactance curve for a resistor and capacitor connected in parallel. The arrow shows the direction of the increasing frequency.

It is possible to distinguish three regimes from the conductivity versus frequency plot[3] (Figure 11) (60). The first regime is in the low frequency I and can be attributed to the electrode polarization. In the middle frequency regime II the conductivity is frequency independent corresponding to DC conductivity.

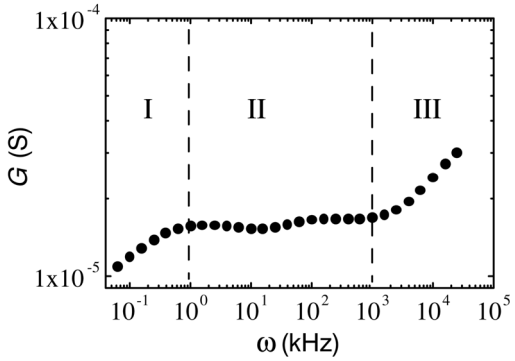

Figure 11. An example of conductance, *G,* [3] as a function of frequency.

[3] Conductance G and conductivity σ are connected by $\sigma = \frac{l}{A} G$, where l is the thickness and A is the cross-sectional area of the sample.

In the high frequency regime III the frequency obeys Jonscher's Universal Power law (61):

$$\sigma(\omega) = \sigma(0) + A\omega^n,$$

where A, n, and $\sigma(0)$ are temperature-dependent material parameters and n is limited to $0 < n < 1$.

Almond and West (62) determined the hopping frequency ω_p of the charge carriers using equation:

$$\omega_p = \left[\frac{\sigma(0)}{A}\right]^{1/n}.$$

ω_p is characteristic frequency associated with the frequency of the dielectric loss peak and it is assumed to be thermally activated (60). The hopping frequency is determined from the point where the conductivity is $\sigma(\omega) = 2\sigma(0)$.

3.3.1. Experimental setup for conductivity measurements

Conductivity measurements were performed at the frequency region 0.01-10 000 kHz (see Articles I-II and V for more details). The Nyqvist plots (i.e. Z', Z'') of the materials showed typical semicircle behavior, which can be described by resistor and capacitor in parallel such as shown in Figure 10. The conductivity was determined at 1 kHz frequency which was found to be in regime II of Figure 11 and corresponds to the DC-resistance of the resistor in the model circuit.

The conductivity measurements in the Articles I and II were performed using measurement chamber illustrated in Figure 12 A. The sample was placed on top of golden electrodes and another glass plate was glued using epoxy in order to exclude the errors due to atmospheric exposure of humidity.

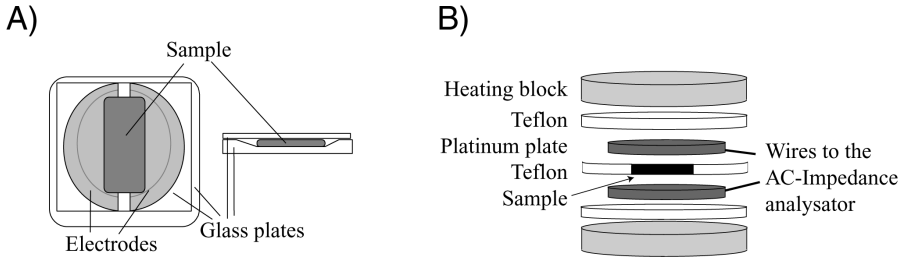

Figure 12. The conductivity measurement setup used in A) Articles I-II and B) Article V.

The conductivity measurements in the Article V were performed in the measurement chamber illustrated in Figure 12 B. In this improved setup the sample was placed between two platinum plates and surrounded with teflon. The heating blocks above and below the sample were insulated from the sample by teflon and the temperature was regulated by Linkam TMS91 temperature controller.

The contact resistance was minimized by heating the samples above the glass transition temperature of the harder part of the material (i.e. PS) before the measurements were performed. The effect of water was minimized by closing the sample.

4. Towards anisotropic conductors based on self-organization

In this Chapter we represent the main results of Articles I-V. We have considered self-organization of polymeric supramolecules with and without protonically conducting structures, applied oscillatory shear flow to achieve alignment of the local self-organized structures and investigated the resulting conductivity properties of the material.

4.1. Conductivity of P4VP(MSA)$_{1.0}$ and P4VP(TSA)$_{1.0}$ polysalt

Protonically conducting materials were discussed in Section 1.3. We have used a method to achieve protonically conducting materials based on acid- base complexes (47, 48). All of the the materials described in Figure 5 contain P4VP which has nitrogen in the aromatic ring. This nitrogen can make ionic bonding with strong acids by accepting a proton. We chose MSA to make our first model material because it is the simplest sulphonic acid. The conductivity is of Arrhenius type with activation energy of 0.51 eV (Figure 13). This polysalt is hard and brittle but as it is very hygroscopic, within 5 minutes under atmospheric conditions the material turns soft due to adsorbed water. In order to minimize the amount of water in the conductivity measurements the P4VP(MSA)$_{1.0}$ was dried at 60°C in vacuum for 24 hrs and stored in desiccator before the measurement. However, we do not expect that completely anhydrous state can be achieved by vacuum drying. When P4VP(MSA)$_{1.0}$ was further complexed with PDP the hygroscopic nature of material was reduced. The resulting material P4VP(MSA)$_{1.0}$PDP$_{1.0}$ (Figure 5 case A) forms a lamellar structure, which becomes disordered above order-disorder transition (ODT) at 100°C.

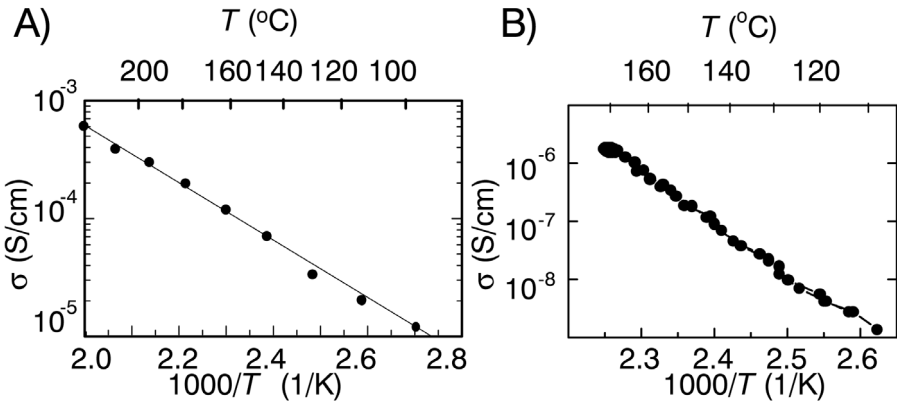

Figure 13. A) Conductivity of P4VP(MSA)$_{1.0}$ as a function of temperature. B) Conductivity of P4VP(TSA) $_{1.0}$ as a function of temperature. The polysalt is made from chloroform.

For the Article V we chose TSA instead of MSA, which was used in Articles I-II. This was due to several reasons. TSA is less hygroscopic and has greater thermal stability which both made shearing at high temperatures for long time possible. The formed complexes $P4VP(TSA)_{1.0}PDP_{1.0}$ (Figure 5) had higher order-disorder transition temperatures (140°C) than complexes made from MSA (100°C). This made the alignment under the shear flow possible both above and below the order-disorder transition temperature of $P4VP(TSA)_{1.0}PDP_{1.0}$. In addition, the phase behavior of PS-*block*-$P4VP(TSA)_{1.0}PDP_{1.0}$ was less complicated than of PS-*block*-$P4VP(MSA)_{1.0}PDP_{1.0}$ which made the TSA based sample easier to handle.

The conductivity of $P4VP(TSA)_{1.0}$ as a function of temperature is presented in Figure 13. The conductivity of the polymer salt $P4VP(TSA)_{1.0}$ is improved when the degree of crystallinity of the salt was reduced. Two solvents were used to prepare the samples: dimethylformamide (DMF) and methanol. Because of the high boiling point of DMF, it cannot be fully extracted from the material and thus it acts as a plasticizer. It is well known from the literature that plasticizers reduce the crystallinity of the materials and thus enhance the conductivity (43, 46, 63). Indeed, the conductivity was found to be 4 decades lower in the case of polysalt made from methanol than in the polysalt made from DMF. Also the activation energy was greatly decreased from 1.8 eV to 0.5 eV when the solvent was changed form methanol to DMF.

For $P4VP(TSA)_{1.0}$ the drying procedure is explained in detail in Article V.

4.2. Hierarchical self-organized supramolecules based on $P4VP(MSA)_{1.0}$ polysalt (Articles I and II)

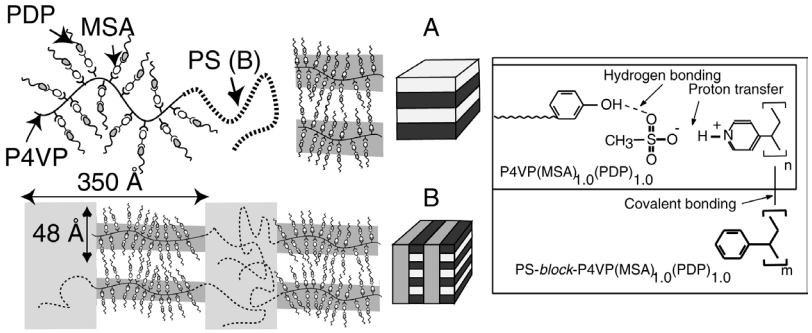

Figure 14. Schematic illustration of $P4VP(MSA)_{1.0}(PDP)_{1.0}$ (case A) and PS-*block*- $P4VP(MSA)_{1.0}(PDP)_{1.0}$ (case B) and their chemical formulas.

The conductivity of the $P4VP(MSA)_{1.0}$ –salt showed a typical Arrhenius kind of behavior with activation energy of 0.51 eV (Figure 13). However, when the self-organized structure is formed in the case of $P4VP(MSA)_{1.0}PDP_{1.0}$ (case A), the conductivity properties are changed. At low temperatures i.e. below 140°C (Figure 15) the conductivity obeys a VTF equation with pseudo activation energy of 0.16 eV and temperature of 199 K. While the temperature is further raised and a macrophase separation occurs (Figure 2 of Article I) the conductivity drops suddenly as shown in Figure 15. This is probably due PDP forming insulating areas hindering the conducting pathways. When the material becomes miscible but disordered around 190°C, the conductivity starts to increase again.

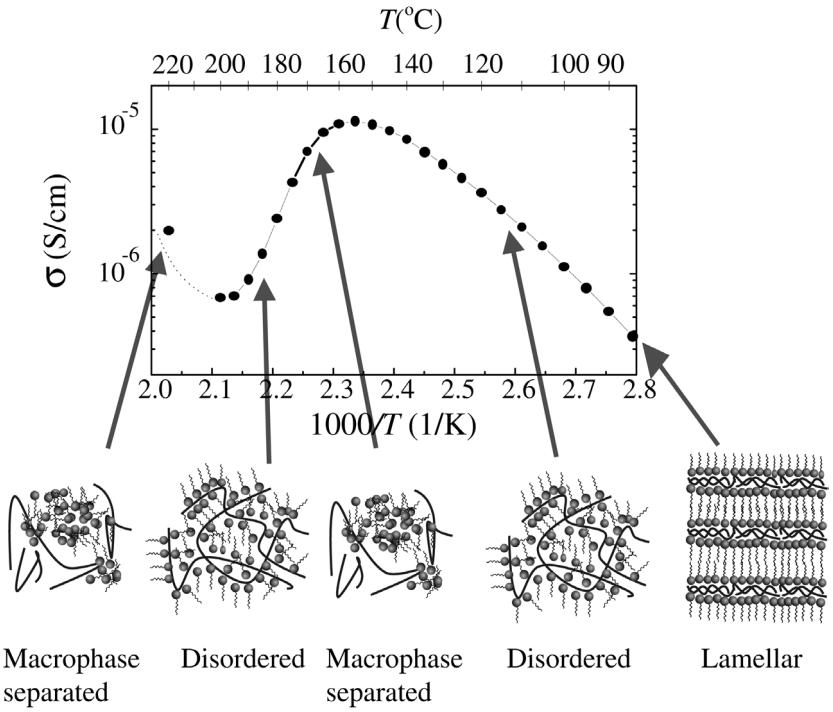

Figure 15. Conductivity of P4VP(MSA)$_{1.0}$PDP$_{1.0}$ as a function of temperature

The achievement of the hierarchical order makes also the conductivity behavior more complex. In the PS-*block*-P4VP(MSA)$_{1.0}$PDP$_{1.0}$ when the molecular weights have been properly selected. There is a larger lamellar structure between PS and P4VP(MSA)$_{1.0}$PDP$_{1.0}$ and a smaller lamellar structure inside of the P4VP(MSA)$_{1.0}$PDP$_{1.0}$ (Figure 14 case B). Using related materials it was found by TEM that the smaller structure tends to orient perpendicular to the large structure (Article I).

The changes of such hierarchical structures are presented in detail in Article I. The schematic pictures of the phases as a function of temperature are presented in Figure 16 together with the conductivity data. At low temperatures the conductivity is along the nanoslabs of P4VP(MSA)$_{1.0}$. Upon heating, the conductivity of PS-*block*-P4VP(MSA)$_{1.0}$PDP$_{1.0}$ increases suddenly when the order-disorder transition (ODT) of the small structure (i.e. P4VP(MSA)$_{1.0}$PDP$_{1.0}$) appears (Figure 16). Now the conductivity is along the layers of P4VP(MSA)$_{1.0}$PDP$_{1.0}$. When the temperature is further raised, the hydrogen bonds become weaker and at the same time the PDP becomes miscible in the polystyrene domains. As a result the structure is changed into the cylindrical morphology with conductivity along the cylinders. This conductivity behavior is essentially reversible (Figure 17) during heating and cooling. Because the sample was heated to 220°C the reversibility is not perfect probably due to some degradation.

All the samples were unoriented, which means that the conductivity properties were averages over all three directions. The structure is locally ordered but there is no overall orientation. To distinguish the conductivity properties along the different directions inside the material, it is necessary to achieve globally ordered samples. This is the motivation for the rest of the work.

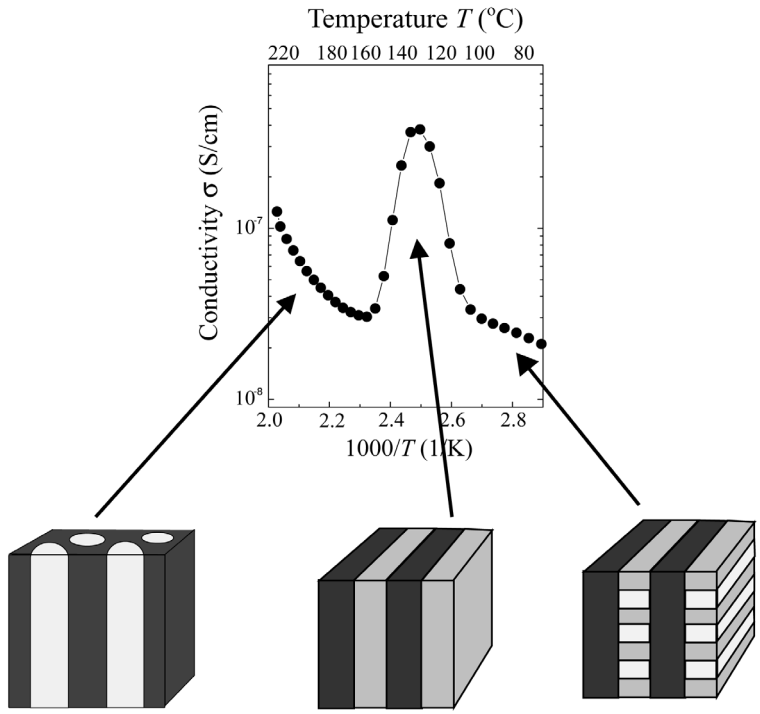

Figure 16. The conductivity behavior of unoriented PS-*block*-P4VP(MSA)$_{1.0}$PDP$_{1.0}$ as a function of temperature. When the temperature is raised first the small structure becomes disordered resulting in an increase in the conductivity. When the temperature is further increased, the amphiphiles become soluble in the PS part and an order-order-transition to a cylindrical phase occurs. The conductivity is decreased due to this phase change.

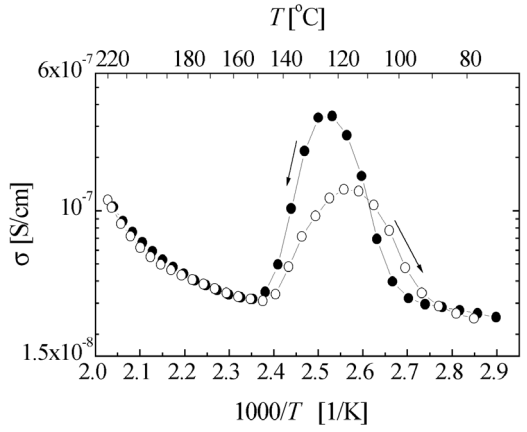

Figure 17. Conductivity of PS- *block* -P4VP(MSA)$_{1.0}$PDP$_{1.0}$ at 1 kHz. Heating is illustrated in solid symbol and cooling with open symbol. Reproduced with permission from Synthetic Metals, 1999, 102, 1498-1501 (Article II).

4.3. Macroscopically aligned hierarchical self-organized structures (Article III)

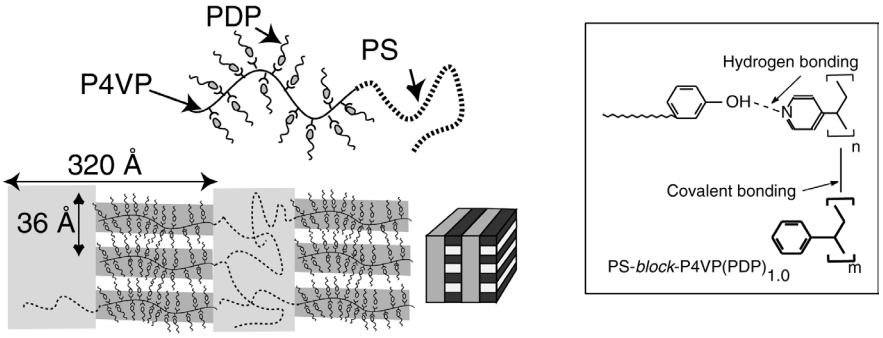

Figure 18. Schematic illustration of PS-*block*-P4VP(PDP)$_{1.0}$ and its chemical formula.

The first effort towards well-aligned hierarchical materials was performed using PS-*block*-P4VP(PDP)$_{1.0}$. This material reminds PS-*block*-P4VP(MSA)$_{1.0}$PDP$_{1.0}$ considered in Articles I-II but it is without the acid and therefore not conducting. The block lengths were selected to have the lamellar-*within*-lamellar structure. The larger structure was formed between PS and P4VP(PDP)$_{1.0}$ and the smaller structure was inside P4VP(PDP)$_{1.0}$ (Figure 18). The material was shear flow aligned above the ODT of the small structure in order to achieve a well-aligned large structure. When the sample was cooled down, the small structure ordered perpendicular to the large structure. The SAXS patterns of the sample before and after shear are presented in Figure 19. Before shearing the sample was poorly aligned. After shearing the overall order is increased: higher orders are observable and the intensities of the peaks are greatly increased. However, the small structure remained unaligned. It is at right angles to the large structure but has all the possible alignments (Figure 19 D).

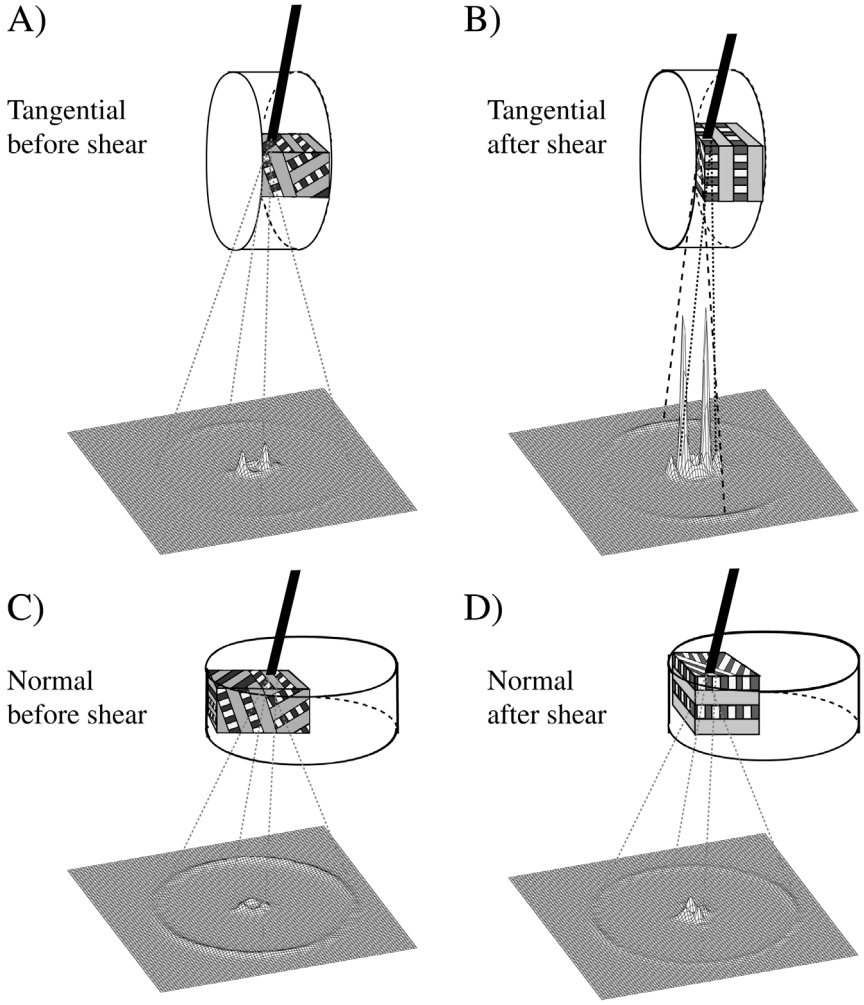

Figure 19. SAXS patterns of PS-*block*-P4VP(PDP)$_{1.0}$ and schematic illustrations of the alignment before and after shear in the tangential and the normal directions. After shearing the larger structure is aligned parallel whereas the smaller structure is at right angles to the large structure but has all the possible alignments, as is clear from the schematic picture in D.

4.4. Self-organized supramolecules in the shear flow (Article IV)

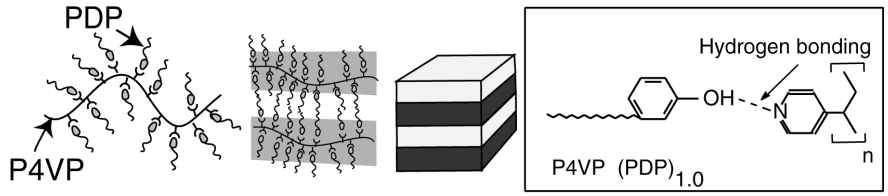

Figure 20. Schematic illustration of P4VP(PDP)$_{1.0}$ and its chemical formula

To understand shearing of hierarchical structure we needed more insight into the smaller lamellar structure based on the physical bonds of the amphiphiles i.e. how hydrogen bonded system behaves under the oscillatory shear flow.

The properties of block copolymers (23, 27, 32, 35, 64, 65) and related side chain liquid crystalline polymers (38, 40, 66) have been widely studied. The alignment diagrams have been presented for PS-PI and PEP-PEE (see Introduction) (23). We studied the hydrogen-bonded comb shaped polymer, P4VP(PDP)$_{1.0}$, which forms lamellar structures. The material was imposed to the oscillatory shear flow and the results were compared with the studies of block copolymers and side chain liquid crystalline polymers.

P4VP(PDP)$_{1.0}$ turned out to have somewhat similar shear flow behavior as block copolymers and side chain liquid crystalline polymers. In the linear region the material obeyed time-temperature superposition and the parameters based on WLF[4] equation were in agreement with the results of side chain liquid crystalline polymers (see Article IV for details).

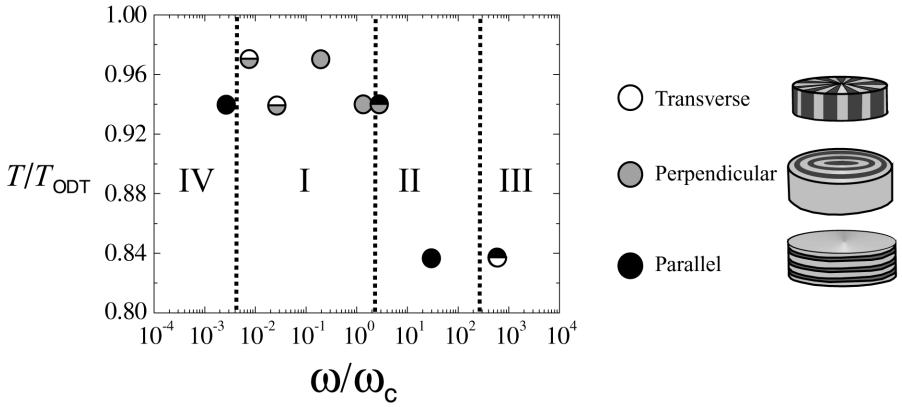

Figure 21. The alignment diagram for P4VP(PDP)$_{1.0}$. Reproduced with permission from Macromolecules, 2001, 34, 2892-2900 (Article IV). Copyright 2001 Am. Chem. Soc.

[4] WLF= Williams, Landel and Ferry

In Article IV, an alignment diagram for P4VP(PDP)$_{1.0}$ is presented (Figure 21). Depending on the temperature, amplitude, and frequency, P4VP(PDP)$_{1.0}$ shows all the three possible alignments, which have been found for diblock copolymers. The observed frequency regimes of the alignments were close to the behavior of diblock copolymers.

In the low frequency regime the materials responded to the flow field of low strain exceptionally well, resulting transverse orientation. This contrasts some of the studies of block copolymers and side chain liquid crystalline polymers. However, when the strain was increased the alignment turned into perpendicular, as expected based on the behavior of block copolymers.

4.5. Macroscopically aligned hierarchical self-organized supramolecules based on P4VP(TSA)$_{1.0}$ polysalt showing anisotropic conductivity (Article V)

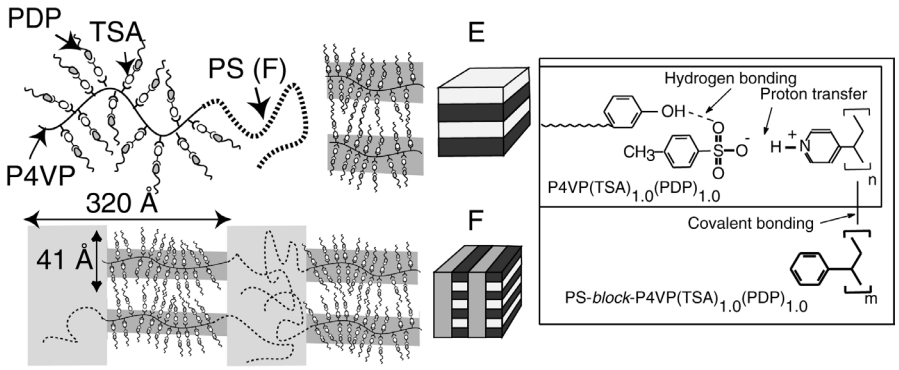

Figure 22. Schematic illustration of P4VP(TSA)$_{1.0}$(PDP)$_{1.0}$ (case E) and PS-*block*- P4VP(TSA)$_{1.0}$(PDP)$_{1.0}$ (case F) and their chemical formulas.

To achieve globally anisotropic conductive materials, the locally self-organized conducting and insulating domains have to be aligned. Previously people have studied layered materials where the conductivity is anisotropic in directions perpendicular and parallel to the layers (67). Various blending processes have been used to achieve anisotropy (68, 69). Also rod-like materials have been studied with several aligning methods (70-72).

PS-*block*-P4VP(TSA)$_{1.0}$PDP$_{1.0}$ was chosen as our model material for anisotropic conductor due to several reasons described earlier in this Thesis. Before concentrating on the conductivity of the aligned hierarchical structure we studied the conductivity of the aligned comb-shaped supramolecular structure i.e. P4VP(TSA)$_{1.0}$PDP$_{1.0}$ (Figure 22 case E) (73). The conductivity measurements for P4VP(TSA)$_{1.0}$PDP$_{1.0}$ were performed using three heating and cooling cycles where the first cycle was below the T_{ODT} (i.e. 50°C – 120°C – 60°C), the second cycle was from 60°C – 160°C – 60°C reaching temperatures above the T_{ODT} and the third cycle was from 60°C – 160°C – 60°C. The conductivity was studied in three different directions i.e. tangential, normal and radial. According to SAXS, the P4VP(TSA)$_{1.0}$PDP$_{1.0}$ structure was aligned parallel to the shearing plates (Article V).

In subsequent conductivity measurements we found that if the temperature was kept below the T_{ODT} (i.e. 140°C) the conductivity was reversible in all the three directions (Figure 23 A and Figure 24 A and B) during the temperature cycles. The conductivities obeyed the VTF equation with a pseudo activation energy of 0.11-0.13 eV with T_0 = 199K.

Upon heating above the T_{ODT} of the structure, the conductivity level was increased in the normal direction (Figure 23 B). The increase of conductivity was found in all the conductivity measurements in the normal direction and can be connected to loss of alignment. During repeated cycles before the first heating above T_{ODT} the conductivity is measured across the insulating layers (scheme in Figure 23 A). When the sample is heated above the T_{ODT} the structure looses its orientation and therefore the conductivity *increases* (Figure 23 B).

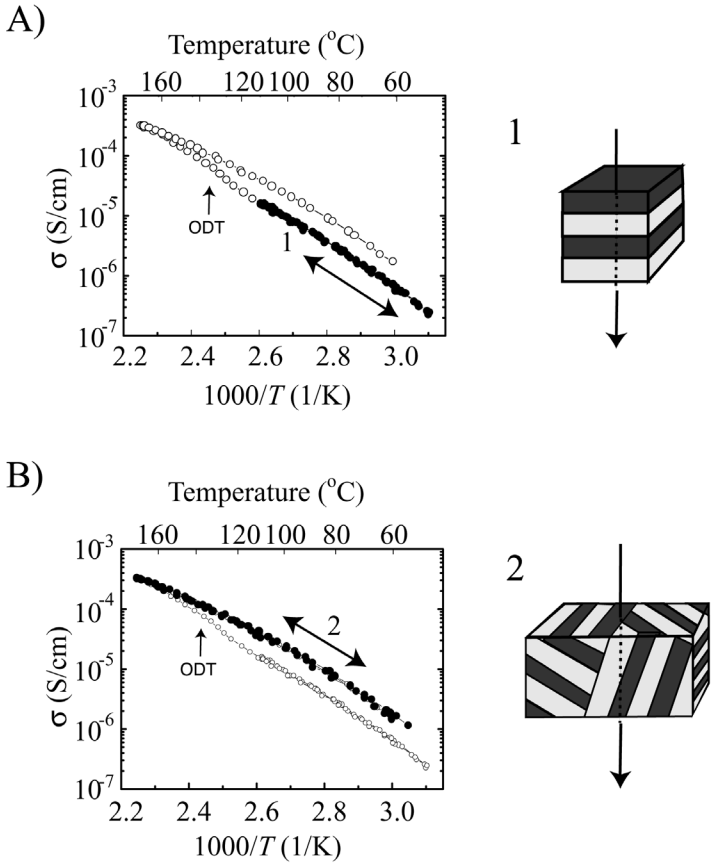

Figure 23. Conductivity of P4VP(TSA)$_{1.0}$PDP$_{1.0}$ in the normal direction for a shear oriented sample. A) The solid dots represent the conductivity in heating cycle below T_{ODT}. The open dots represent the conductivity during the first heating above the T_{ODT} and the cooling thereafter. B) The solid dots represent the subsequent conductivity cycles after the first heating above the T_{ODT}. In this case the conductivity is again reproducible at this slightly higher level probably because the protonically conducting lamellae may not be primarily oriented perpendicular to the measurement direction. So far, we do not yet have the SAXS data to confirm the latter hypothesis.

Due to the parallel alignment we expected that the conductivities would be similar in the tangential and the radial directions. The conductivities were found to remain the same or they were *reduced* (Figure 24 A and B) in contrast to the normal direction, where the conductivity was observed to increase. In conclusion, as full reproducibility in the tangential and radial directions was not yet achieved (probably due to problems with inserting the samples to the sample chamber without causing deformations), we regard the above observations still preliminary and qualitative.

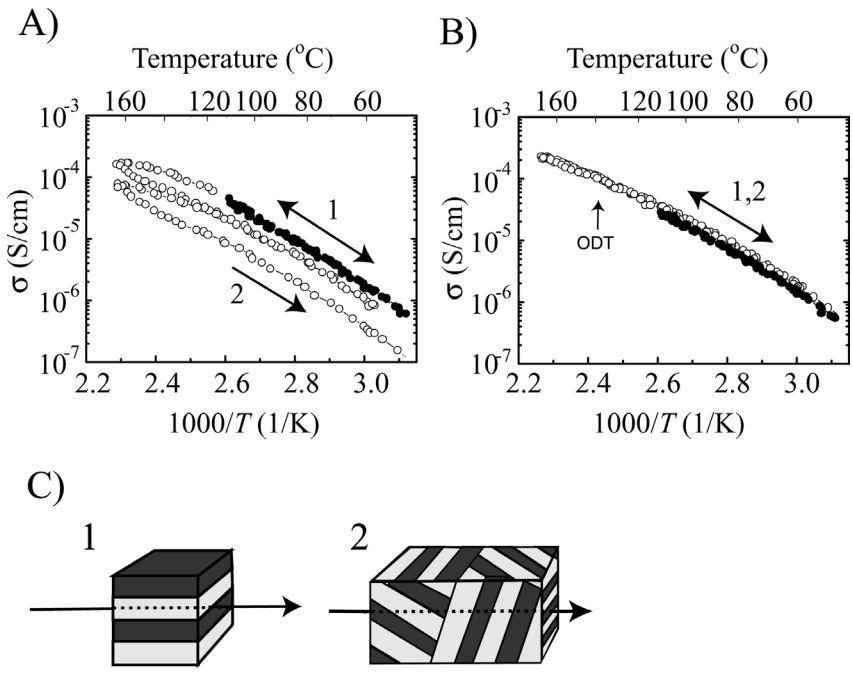

Figure 24. Conductivity of P4VP(TSA)$_{1.0}$PDP$_{1.0}$ in A) radial and B) tangential directions. The solid dots represent the conductivity cycles before the first heating above the T_{ODT} and open dots represents the conductivity after the first heating above the T_{ODT}. Figure C) shows scheme of aligned and not aligned structure.

Instead the subsequent data deals with a more "coarse" behavior, which allows quantitative analysis. Applying the Joncher's universal law (61) to the frequency-conductivity data it was possible to determine the hopping frequencies in the different directions below the T_{ODT} (Figure 25). The hopping rates of P4VP(TSA)$_{1.0}$PDP$_{1.0}$ are equal in the tangential and radial directions whereas the hopping rate is reduced in the normal direction. At temperatures close and above the T_{ODT}, ω_p shifted to frequencies above our measurement window. Similar temperature dependency has also been reported in the literature using different materials (60).

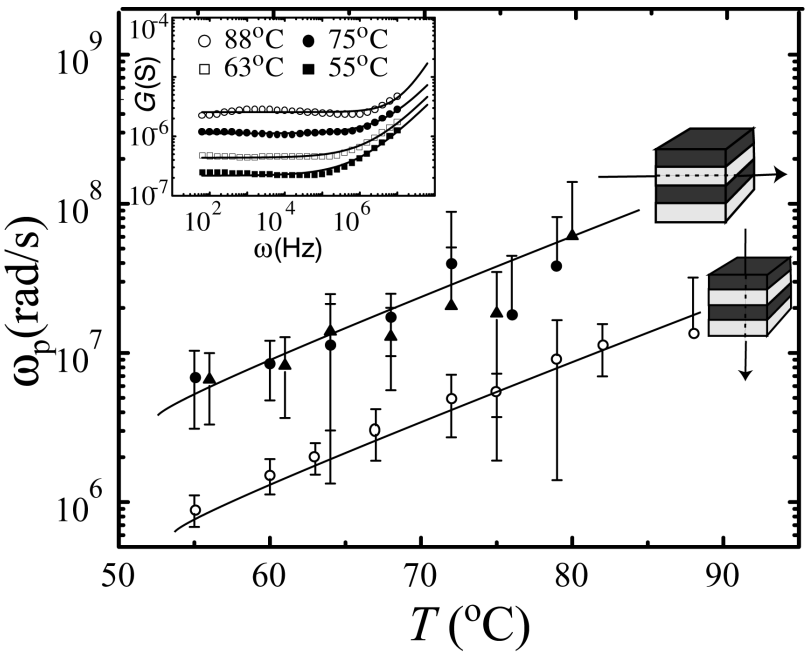

Figure 25. Hopping rate of P4VP(TSA)$_{1.0}$PDP$_{1.0}$ along the conducting layers and perpendicular to them. In the inset there is the conductance (*G)* as a function of frequency at various temperatures.

When hierarchy was additionally invoked to the structure (Figure 22 case F) i.e. PS-*block*-P4VP(TSA)$_{1.0}$PDP$_{1.0}$ the conductivity level was lower in the poorly aligned sample (Figure 26) as compared to the conductivity level of P4VP(TSA)$_{1.0}$(PDP)$_{1.0}$, However, after the two-stage aligning process, where the larger structure was first aligned above the T_{ODT} of the smaller structure and then below T_{ODT} of the smaller structure (see Article V for details) the conductivity level was enhanced to the same level as for the P4VP(TSA)$_{1.0}$(PDP)$_{1.0}$ in spite of its lower concentration. The conductivity has the highest value along the aligned conducting nanoslabs (Figure 26 case 1) and the lowest value across the insulating PS layers (Figure 26 case 3).

The hopping rates presented in Figure 27 are in agreement with the conductivity data. The hopping rate has the largest value along the direction of the conducting nanoscale slabs and smallest across the insulating PS layers. In PS-*block*-P4VP(TSA)$_{1.0}$PDP$_{1.0}$ the value of ω_p increases as the temperature is raised. At high temperatures we were not able to determine ω_p because its value had shifted away from the measurement region.

The anisotropy in the values is not large, but it is clear. By selecting other materials it may be possible to increase the difference in conductivity between the insulating and conducting directions. This study shows that it is possible to achieve tridirectionally anisotropic materials in relatively straightforward way in soft polymeric materials.

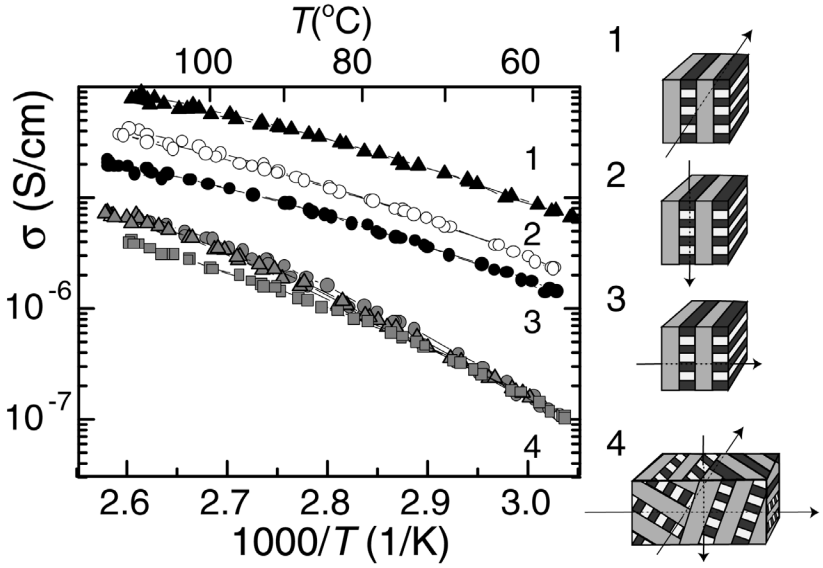

Figure 26. The conductivity of PS-*block*-P4VP(TSA)$_{1.0}$PDP$_{1.0}$ as a function of 1/*T*. The corresponding measurement directions are also shown. Case 4 represents the conductivity of poorly aligned structure.

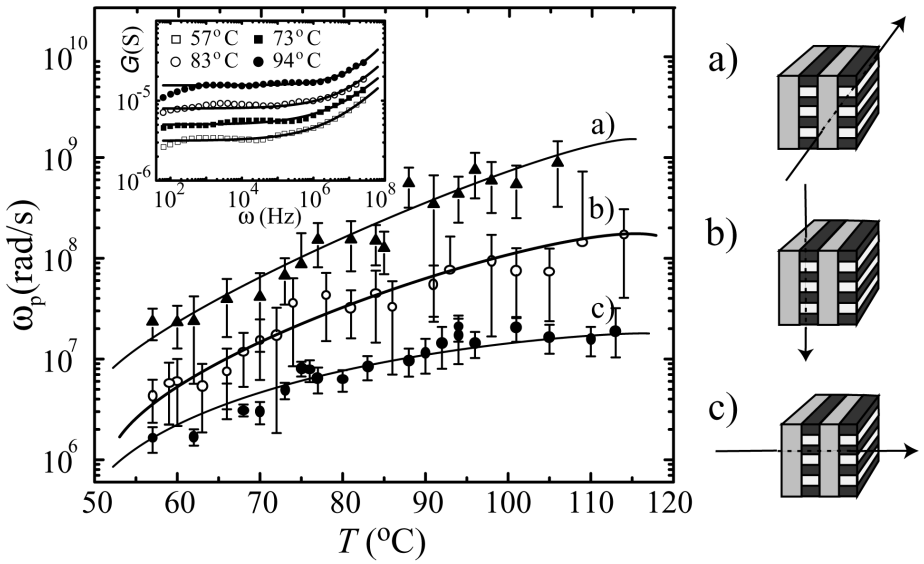

Figure 27. The hopping rates of PS- *block* -P4VP(TSA)$_{1.0}$PDP$_{1.0}$ as a function of temperature. In the inset there is the conductance (*G)* as a function of frequency at various temperatures.

5. "Hairy tubes" – a route towards mesoporous materials with functional surfaces (Article VI)

Finally we show another scheme to use the self-organized materials of this Thesis. We represent our method to achieve mesoporous materials (Article VI) based on selective solvent and the physical nature of hydrogen bonds.

5.1. Shear flow alignment of the asymmetric PS-*block*-P4VP(PDP)$_{1.0}$ structures

Asymmetric block copolymer structures under shear flow have been investigated using poly(ethylene propylene)-*block*-poly(ethylethylene), PEP-PEE, where PEP formed the stiff matrix and PEE soft rods inside it (74-78). It was suggested that mechanical contrast plays an important role in alignment of the cylinders. It was easier to align a soft material in a stiff matrix than vice versa. As a result the cylinders were aligned along the shear flow.

For Article VI the block lengths were chosen to obtain lamellar-*within*-cylinders structure, where PS forms the matrix with P4VP(PDP)$_{1.0}$ rods inside (Figure 28). Because PDP decreases the glass transition temperature of the P4VP block to below room temperature (79) whereas the polystyrene part softens around 90°C, our material is in some sense similar to PEP-PEE. At the shearing temperatures 120°C, the polystyrene forms the stiff matrix with soft rods of P4VP(PDP)$_{1.0}$ aligned along the shear flow.

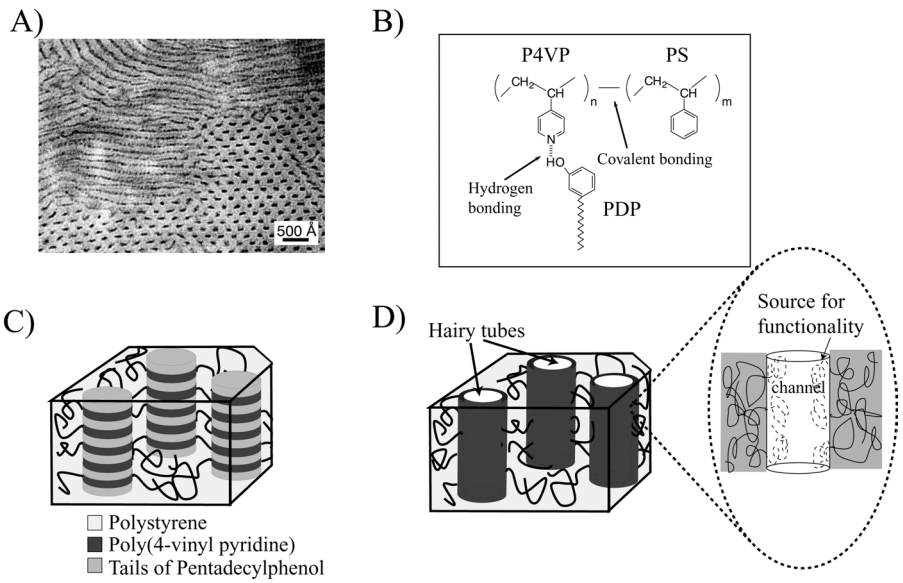

Figure 28. A procedure to prepare hairy tubes. A) A TEM image of lamellar-*within*-cylinder structure (15), B) chemical formulas and C) a schematic illustration of the structure. D) An illustration of the structure after amphiphile removal leading to P4VP brushes at the walls of the hollow cylinders i.e. so-called hairy tubes. TEM by J. Ruokolainen.

5.2. Nanoporous materials

A lot of research is done in the field of nanoporous (or equivalently mesoporous) materials (for different methods see the introduction of Article VI). For example nanoporous materials (pore size 20-500 Å) have been prepared from block copolymers via photo-crosslinking and ozonolysis (80). On the other hand, materials have been constructed using assemblies of surfactants and block copolymers in the synthesis of inorganic materials (81-83). Different kinds of degradation processes have been presented to obtain nanoporosity (84, 85). A new application has been to prepare so-called low dielectric material for electronics, based on self-assembly and selective removal of materials (86, 87).

In our case we can exploit the physical nature of the hydrogen bonds. Because they are not permanent, it is possible to remove the side chains afterwards particularly easily resulting in a controllable porosity inside of the material. This method is relatively straightforward producing material with pores with high density of polymer chains at the walls. The concept is versatile with the additional possibility to functionalize the inner wall of the pores.

We have used the concept further to prepare other types polymeric nano-objects, nanofibers by applying the same method to material with opposite i.e. cylinders-*within*-lamellar structure. (88)

6. Discussion

In this Thesis we study nanopatterned polymeric materials based on self-organization of comb-shaped supramolecules. We induce overall alignment of the structures, thus leading to materials that allow control of protonic conductivity in three dimensions as well as nanoporous materials.

We started with protonically conducting hierarchically self-organized supramolecules with a peculiar conductivity behavior. This structure is, however, not macroscopically aligned and therefore the conductivity is isotropic throughout the sample. In order to macroscopically align the nanostructures and to study the conductivity along the different orientations we have investigated the structures under a shear flow.

First alignment efforts were performed with using the simple hierarchical self-organized supramolecular material, i.e. lamellar-*within*-lamellar structure, without protonically conducting salts. Then we proceeded to investigate the inner structure of this hierarchical material based on hydrogen-bonded amphiphiles under an oscillatory shear flow. We constructed an alignment diagram and compared the results with knowledge from block copolymers and side chain liquid crystalline polymers.

Finally we have presented macroscopically aligned protonically conducting hierarchical self-organized supramolecules, which are globally tridirectional conductors with anisotropic hopping conductivity. Both the smaller and the larger structures are first shear flow oriented. The conductivity of this hierarchically structured material is analyzed and it is found that the oriented nanostructures reflect the global conductivity. The conductivity has the lowest value in the insulating direction and the highest value in the conducting direction. So far the conductivity level in our model material was not high compared to the best existing protonic conductors, but it demonstrates that the manipulation of conductivity is possible using nanostructures.

In the end, we briefly studied asymmetric structures i.e. lamellae inside of cylinders and found a method to achieve mesoporous materials. We imposed the material containing hydrogen-bonded amphiphiles in selective solvent and rinsed off the amphiphiles. The resulting material consists of a solid polymer matrix with polymer hairs on the walls of empty cylinders.

The results of this Thesis show that materials, which are relatively simple to produce, allow tailored properties due to their aligned self-organized nanoscale structure. In order to produce large amounts of aligned material some other methods than oscillatory flow are desirable. Such methods might be electric or magnetic field that suggests a logical continuation of the topics discussed in this Thesis.

References

1. Brostow, W. Ed., *Mechanical and Thermophysical Properties of Polymer Liquid Crystals*, Chapman & Hall, 1998.
2. Hamley, I. W. *The Physics of Block Copolymers*, Oxford University Press, Oxford, 1998.
3. Antonietti, M., Conrad, J. and Thünemann, A., *Polyelectrolyte-Surfactant Complexes: A New Type of Solid Mesomorphous Material,* Macromolecules, **1994**, *27***,** 6007.
4. Ober, C. and Wegner, G., *Polyelectrolyte-Surfactant Complexes in the Solid State: Facile Building Blocks for Self-Organizing Materials,* Advanced Materials, **1997**, *9***,** 17-31.
5. ten Brinke, G. and Ikkala, O., *Ordered Structures in Molecular Bottlebrushes,* Trends in Polymer Science, **1997**, *5***,** 213.
6. Antonietti, M., Wenzel, A. and Thünemann, A., *The "Egg-Carton" Phase: a New Morphology of Complexes of Polyelectrolytes with Natural Lipid Mixtures,* Langmuir, **1996**, *12***,** 2111-2114.
7. Antonietti, M., Conrad, J. and Thünemann, A., *Polyelectrolyte-Surfactant Complexes: A New Class of Highly Ordered Polymer Materials,* Trends in Polymer Science, **1997**, *5***,** 262.
8. Ruokolainen, J., Tanner, J., ten Brinke, G., Ikkala, O., Torkkeli, M. and Serimaa, R., *Poly(4-vinylpyridine)/Zinc Dodecyl Benzene Sulphonate. Mesomorphic State due to Coordination Complexation,* Macromolecules, **1995**, *28***,** 7779.
9. Ruokolainen, J., Torkkeli, M., Serimaa, R., Komanschek, E., Ikkala, O. and ten Brinke, G., *Order-Disorder Transitions in Polymer-Surfactant Systems,* Physical Review E, **1996**, *54***,** 6646.
10. Ruokolainen, J., ten Brinke, G., Ikkala, O., Torkkeli, M. and Serimaa, R., *Mesomorphic Structures in Flexible Polymer-Surfactant Systems Due to Hydrogen Bonding: Poly(4-vinylpyridine)-Pentadecylphenol,* Macromolecules, **1996**, *29***,** 3409.
11. Ruokolainen, J., Mäkinen, R., Torkkeli, M., Mäkelä, T., Serimaa, R., ten Brinke, G. and Ikkala, O., *Switching Supramolecular Polymeric Materials with Multiple Length Scales,* Science, **1998**, *280***,** 557-560.
12. Ruokolainen, J., Torkkeli, M., Serimaa, R., Komanschek, B. E., ten Brinke, G. and Ikkala, O., *Order-Disorder Transition in Comb-like Copolymers Obtained by Hydrogen Bonding Between Homopolymers and End-Functionalized Oligomers: Poly(4-vinyl pyridine) - Pentadecyl Phenol,* Macromolecules, **1997**, *30***,** 2002.
13. Ruokolainen, J., Tanner, J., Ikkala, O., ten Brinke, G. and Thomas, E. L., *Direct Imaging of Self-Organized Comb Copolymer-like Systems Obtained by Hydrogen Bonding: Poly(4-vinyl pyridine)-4-Nonadecylphenol,* Macromolecules, **1998**, *31***,** 3532-3536.
14. Ruokolainen, J., Saariaho, M., Ikkala, O., ten Brinke, G., Thomas, E. L., Torkkeli, M. and Serimaa, R., *Supramolecular Routes to Hierarchical Structures: Comb-Coil Diblock Copolymers Organized With Two Length Scales,* Macromolecules, **1999**, *32***,** 1152-1158.
15. Ruokolainen, J., ten Brinke, G. and Ikkala, O. T., *Supramolecular Polymeric Materials with Hierarchical Structure-Within-Structure Morphologies,* Advanced Materials, **1999**, *11***,** 777.

16. Mansky, P., DeRouchey, J., Russell, T. P., Mays, J., Pitsikalis, M., Morkved, T. and Jaeger, H., *Large-Area Domain Alignment in Block Copolymer Thin Films Using Electric Fields,* Macromolecules, **1998**, *31***,** 4399-4401.
17. Thurn-Albrecht, T., Schotter, J., Kästle, G. A., Emley, N., Shibauchi, T., Krusin-Elbaum, L., Guarini, K., Black, C. T., Tuominen, M. T. and Russell, T. P., *Ultrahigh-Density Nanowire Arrays Grown in Self-Assembled Diblock Copolymer Templates,* Science, **2000**, *290***,** 2126-2129.
18. Finkelmann, H., Naegele, D. and Ringsdorf, H., *Orientation of Nematic Liquid Crystalline Polymers in the Electric Field,* Makromolecular Chemistry, **1979**, *180***,** 803-806.
19. Gurovich, E., *Why Does an Electric Field Align Structures in Copolymers?,* Physical Review Letters, **1995**, *74***,** 482-485.
20. Sata, H., Kumura, T., Ogawa, S., Yamato, M. and Ito, E., *Magnetic Orientation of Poly(ethylene-2,6-naphthalate),* Polymer, **1996**, *37***,** 1879-1882.
21. Gupta, V. K., Krishnamoorti, R., Kornfield, J. A. and Smith, S. D., *Evolution of microstructure during shear alignment in a polystyrene-polyisoprene lamellar diblock copolymer,* Macromolecules, **1995**, *28***,** 4464-4474.
22. Zhang, Y., Wiesner, U. and Spiess, H. W., *Frequency Dependence of Orientation in Dynamically Sheared Diblock Copolymers,* Macromolecules, **1995**, *28***,** 778-781.
23. Chen, Z.-R. and Kornfield, J. A., *Flow-Induced Alignment of Lamellar Block Copolymer Melts,* Polymer, **1998**, *39***,** 4679-4699.
24. Koppi, K. A., Tirrell, M., Bates, F. S., Almdal, K. and Colby, R. H., *Lamellae orientation in dynamically sheared diblock copolymer melts,* Journal of Physics II France, **1992**, *2***,** 1941-1959.
25. Koppi, K. A., Tirrell, M. and Bates, F. S., *Shear-Induced Isotropic-to-Lamellar Transition,* Physical Review Letters, **1993**, *70***,** 1449-1452.
26. Kannan, R. M. and Kornfield, J. A., *Evolution of Microstructure and Viscoelasticity during Flow Alignment of a Lamellar Diblock Copolymer,* Macromolecules, **1994**, *27***,** 1177-1186.
27. Winey, K., Patel, S. S., Larson, R. G. and Watanabe, H., *Morphology of a Lamellar Diblock Copolymer Aligned Perpendicular to the Sample Plane: Transmission Electron Microscopy and Small-Angle X-ray Scattering,* Macromolecules, **1993**, *26***,** 4373-4375.
28. Chen, Z.-R., Issaian, A. M., Kornfield, J. A., Smith, S. D., Grothaus, J. T. and Satkowski, M. M., *Dynamics of Shear-Induced Alignment of a Lamellar Diblock: A Rheo-optical, Electron Microscopy and X-ray Scattering Study,* Macromolecules, **1997**, *30***,** 7096-7114.
29. Gupta, V. K., Krishnamoorti, R., Kornfield, J. A. and Smith, S. D., *Role of Strain in Controlling Lamellar Orientation during Flow Alignment of Diblock Copolymers,* Macromolecules, **1996**, *29***,** 1359 -1362.
30. Gupta, V. K., Krishnamoorti, R., Chen, Z.-R., Kornfield, J. A., Smith, S. D., Satkowski, M. M. and Grothaus, J. T., *Dynamics of Shear Alignment in a Lamellar Diblock Copolymer: Interplay of Frequency, Strain Amplitude and Temperature,* Macromolecules, **1996**, *29***,** 875-884.

31. Zhang, Y. and Wiesner, U., *Symmetric diblock copolymers under large amplitude oscillatory shear flow: Entanglement effect,* Journal of Chemical Physics, **1995**, *103***,** 4784-4793.
32. Chen, Z.-R., Kornfield, J. A., Smith, S. D., Grothaus, J. T. and Satkowski, M. M., *Pathways to macroscale order in nanostructured block copolymers,* Science, **1997**, *277***,** 1248-1253.
33. Zhang, Y., Wiesner, U., Yang, Y., Pakula, T. and Spiess, H. W., *Annealing Effects on orientation in Dynamically Sheared Diblock Copolymers,* Macromolecules, **1996**, *29***,** 5427-5431.
34. Zhang, Y. and Wiesner, U., *Symmetric diblock copolymers under large amplitude oscillatory shear flow: dual frequency experiments,* Journal of Chemical Physics, **1997**, *106***,** 2961-2969.
35. Zhang, Y. and Wiesner, W., *Rheology of lamellar polystyrene-block-polyisoprene diblock copolymers,* Macromolecular Chemistry and Physics, **1998**, *199***,** 1771-1784.
36. Maring, D. and Wiesner, U., *Threshold strain value for perpendicular orientation in dynamically sheared diblock copolymers,* Macromolecules, **1997**, *30***,** 660-662.
37. Wiesner, U., *Lamellar diblock copolymers under large amplitude oscillatory shear flow: order and dynamics,* Macromolecular Chemistry and Physics, **1997**, *198***,** 3319.
38. Kannan, R. M., Kornfield, J. A., Schwenk, N. and Boeffel, C., *Shear-Induced Orientation of Side-Group Liquid Crystalline Polymers,* Advanced Materials, **1994**, *6***,** 214-216.
39. Wiberg, G., Skytt, M.-L. and Gedde, U. W., *Shear induced alignment and relaxation of orientation in smectic side-chain liquid-crystalline polymers,* Polymer, **1998**, *39***,** 2983-2986.
40. Hamley, I. W., Davidson, P. and Gleeson, A. J., *Shear-induced layer alignment in the smectic phase of a side chain liquid crystal polymer,* Polymer, **1999**, *40***,** 3599-3603.
41. Osuji, C., Zhang, Y., Mao, G., Ober, C. K. and Thomas, E. L., *Transverse Cylindrical Microdomain Orientation in an LC Diblock Copolymer under Oscillatory Shear,* Macromolecules, **1999**, *32***,** 7703-7706.
42. Rubin, S., Kannan, R. M., Kornfield, J. A. and Boeffel, C., *Effect of Mesophase Order and Molecular Weight on the Dynamics of Nematic and Smectic Side-Group Liquid Crystalline Polymers,* Macromolecules, **1995**, *28***,** 3521-3530.
43. Ferry, A. and Doeff, M. M., *Polymer Electrolytes- Self-organization and Ionic Transport Properties,* Current Trends in Polymer Science, **1998**, *3***,** 117-130.
44. Armand, M. B. in *Polymer Electrolyte Reviews 1*, eds. MacCallum, J. R. & Vincent, C. A.,Elsevier Applied Science, London and New York, 1987, pp. 1-22.
45. Watanabe, M. and Ogata, N. in *Polymer Electrolyte Reviews 1*, eds. MacCallum, J. R. & Vincent, C. A., Elsevier Applied Science, London and New York, 1987, pp. 39-68.
46. Ruzette, A.-V. G., Soo, P. S., Sadoway, D. R. and Mayes, A. M., *Melt-Formable Block Copolymer Electrolytes for Lithium Rechargeable Batteries,* Journal of Electrochemical Society, **2001**, *148***,** A537-A543.

47. Kerres, J., *Development of Ionomer Membranes for Fuel Cells,* Journal of Membrane Science, **2001**, *185***,** 3-27.
48. Rikukawa, M. and Sanui, K., *Proton-conducting Polymer Electrolyte Membranes Based on Hydrocarbon Polymers,* Progress in Polymer Science, **2000**, *25***,** 1463-1502.
49. Stankovic, R. I., Lenz, R. W. and Karasz, F. E., *Electrical Conductivity of Poly(butadiene-co-vinyl pyridine) Diblock Copolymers Doped with TCNQ,* European Polymer Journal, **1990**, *26***,** 675-681.
50. Stankovic, R. I., Lenz, R. W. and Karatz, F. E., *Electrical Conductivity of Iodine Doped Poly(butadiene-co-2-vinyl pyridine) Diblock Copolymers,* European Polymer Journal, **1990**, *26***,** 359-369.
51. Kreuer, K. D., *On the development of Proton Conducting Polymer Membranes for Hydrogen and Methanol Fuel Cells,* Journal of Membrane Science, **2001**, *185***,** 29-39.
52. Owen, J. in *Comprehensive Polymer Science, The synthesis, Characterization, Reactions & Applications of Polymers*, ed. Allen, G. Pergamon Press, Oxford , 1989, Vol. 2. pp.669-686.
53. Binesh, N. and Bhat, S. V., *VTF to Arrhenius Crossover in Temperature Dependence of Conductivity in (PEG)xNH4ClO4 Polymer Electrolyte,* Journal of Polymer Science B: Polymer Physics, **1998**, *25***,** 1201-1209.
54. Chung, S. H., Such, K., Wieczorek, W. and J.R., S., *An Analysis of Ionic Conductivity in Polymer Electrolytes,* Journal of Polymer Science, Part B, Polymer Physics, **1994**, *32***,** 2733-2741.
55. Ratner, M. A. in *Polymer Electrolyte Reviews 1*, eds. MacCallum, J. R. & Vincent, C. A. Elsevier Applied Science, London and New York, 1987, pp. 173-236.
56. Ferry, A., *Effects of Dynamic Spatial Disorder on Ionic Transport Properties in Polymer Electrolytes based on Poly(Propylene Glycol) (4000),* Journal of Chemical Physics, **1997**, *107***,** 9168-9175.
57. Glipa, X., El Haddad, M., Jones, D. J. and Roziere, J., *Synthesis and Characterisation of Sulfonated Polybenzimidazole: a Highly Conducting Proton Exchange Polymer,* Solid State Ionics, **1997**, *97***,** 323-331.
58. Dang, T. D., Bai, S. J., Heberer, D. P., Arnold, F. E. and Spry, R. J., *Ionic Conductivity of Conjugated Water-Soluble Rigid-Rod Polymers,* Journal of Polymer Science: Part B: Polymer Physics, **1993**, *31***,** 1941-1950.
59. Bonanos, N., *Transport Properties and Conduction Mechanism in High-Temperature Protonic Conductors,* Solid State Ionics, **1992**, *53-56***,** 967-974.
60. Viswanathan, A. and Suthanthiraraj, S. A., *Impedance and Modulus Spectroscopic Studies on the Fast Ion Conducting System CuI-Ag2MoO4,* Solid State Ionics, **1993**, *62***,** 79-83.
61. Jonscher, A. K., *The "Universal" Dielectric Response,* Nature, **1977**, *267***,** 673-679.
62. Almond, D. P., Duncan, G. K. and West, A. R., *The Determination of Hopping Rates and Carrier Concentrations in Ionic Conductors by a New Analysis of AC Conductivity,* Solid State Ionics, **1983**, *8***,** 159-164.
63. Antonietti, M., Maskos, M., Kremer, F. and Blum, G., *Dielectric Relaxation and Conductivity in Polyelectrolyte-Surfactant Complexes,* Acta Polymerica, **1996**, *47***,** 460-465.

64. Winey, K. I., Patel, S. S., Larson, R. G. and Watanabe, H., *Interdependence of Shear Deformations and Block Copolymer Morphology,* Macromolecules, **1993**, *26***,** 2542-2549.
65. Bates, F. S. and Fredrickson, G. H., *Block Copolymer Thermodynamics: Theory and Experiments,* Annual Review of Physical Chemistry, **1990**, *41***,** 525.
66. Kannan, R. M., Kornfield, J. A., Schwenk, N. and Boeffel, C., *Rheology of Side-Group Liquid Crystalline Polymers: Effect of Isotropic-Nematic Transition and Evidence of Flow Alignment,* Macromolecules, **1993**, *26***,** 2050-5056.
67. Nazarenko, S., Hiltner, A. and Baer, E., *Polymer Microlayer Structures with Anisotropic Conductivity,* Journal of Materials Science, **1999**, *34***,** 1461-1470.
68. Gabrielson, L. and Folkes, M. J., *Manufacture of Colloidal Polymer Ellipsoids for Anisotropic Conducting Nano-Composites,* Journal of Materials Science, **2001**, *36***,** 1-6.
69. Gray, F. M., MacCallum, J. R., Vincent, C. A. and Giles, J. R. M., *Novel Polymer Electrolytes Based on ABA Block Copolymers,* Macromolecules, **1988**, *21***,** 392-397.
70. Gattinger, P., Rengel, H., Neher, D., Gurka, M., Buck, M., van de Craats, A. M. and Warman, J. M., *Mechanism of Charge Transport in Anisotropic Layers of Phthalocyanine Polymer,* Journal of Physical Chemistry B, **1999**, *103***,** 3179-3186.
71. Duan, X., Huang, Y., Cul, Y., Wang, J. and Liebler, C. M., *Indium Phosphide Nanowires as Building Blocks for Nanoscale Electronic and Optoelectronic Devices,* Nature, **2001**, *409***,** 66-69.
72. Okahata, Y., Kobayashi, T., Tanaka, K. and Shimomura, M., *Anisotropic Electric Conductivity in an Aligned DNA Cast Film,* Journal of American Chemical Society, **1998**, *120***,** 6165-6166.
73. Mäki-Ontto, R., de Moel, K., Polushkin, E., Alberda van Ekenstein, G., ten Brinke, G. and Ikkala, O., to be published, **2001**.
74. Almdal, K., Bates, F. S. and Mortensen, K., *Order disorder, and fluctuation effects in an asymmetric poly(ethylene-propylene)-poly(ethylethylene) diblock copolymer,* Journal of Chemical Physics, **1992**, *96***,** 9122-9132.
75. Bates, F. S., Koppi, K. A., Tirrell, M., Almdal, K. and Mortensen, K., *Influence of Shear on the Hexagonal-to-Disorder Transition in a Diblock Copolymer Melt,* Macromolecules, **1994**, *27***,** 5934-5936.
76. Hamley, I. W., Gehlsen, M. D., Khandpur, A. K., Koppi, K. A., Rosedale, J. H., Schulz, M. F., Bates, F. S., Almdal, K. and Mortensen, K., *Complex layered phases in asymmetric diblock copolymers,* Journal of Physics II France, **1994**, *4***,** 2161-2186.
77. Almdal, K., Mortensen, K., Koppi, K. A., Tirrell, M. and Bates, F. S., *Isotropic and Anisotropic Composition Fluctuations Close to the Order-to-Disorder Transition in an Asymmetric Diblock Copolymer Melt Subjected to Reciprocating Shear Fields,* Journal of Physics II France, **1996**, *6***,** 617-637.
78. Fredrickson, G. H. and Bates, F. S., *Dynamics of Block Copolymers: Theory and Experiment,* Annual Reviews of Material Science, **1996**, *26***,** 501-550.

79. Luyten, M. C., van Ekenstein, G. O. R. A., ten Brinke, G., Ruokolainen, J., Ikkala, O., Torkkeli, M. and Serimaa, R., *Crystallization and Co-crystallization in Supramolecular Comb Copolymer-like Systems: Blends of Poly(4-vinyl pyridine) and Pentadecylphenol,* Macromolecules, **1999**, *32***,** 4404.
80. Stewart, S. and Liu, G., *Hollow Nanospheres from Polyisoprene-block-poly(2-cinnamoyethyl methacrylate)-block-poly(tert-butyl acrylate),* Chemistry of Materials, **1999**, *11***,** 1048-1054.
81. Krämer, E., Förster, S., Göltner, C. and Antoinetti, M., *Synthesis of Nanoporous Silica with New Pore Morphologies by Templating the Assemblies of Ionic Block Copolymers,* Langmuir, **1998**, *14***,** 2027-2031.
82. Förster, S. and Antonietti, M., *Amphiphilic Block Copolymers in Structure-Controlled Nanomaterial Hybrids,* Advanced Materials, **1998**, *10***,** 195.
83. Ying, J. K., Mehnert, C. P. and Wong, M. S., *Synthesis and Applications of Supramolecular-Templated Mesoporous Materials,* Angewandte Chemie International Edition, **1999**, *38***,** 56-77.
84. Bognitzki, M., Hou, H., Ishaque, M., Frese, T., Hellwig, M., Schwarte, C., Schaper, A., Wendorff, J. H. and Greiner, A., *Polymer, Metal, and Hybrid Nano- and Mesotubes by Coating Degradable Polymer Template Fibers (TUFT Process),* Advanced Materials, **2000**, *12***,** 637-640.
85. Thurn-Albrecht, T., Steiner, R., DeRouchey, J., Stafford, C. M., Huang, E., Bal, M., Tuominen, M., Hawker, C. J. and Russell, T. P., *Nanoscopic Templates from Oriented Block Copolymer Films,* Advanced Materials, **2000**, *12***,** 787-791.
86. Mecerreyes, D., Lee, V., Hawker, C. J., Hedrick, J. L., Wursch, A., Volksen, W., Magbitang, T., Huang, E. and Miller, R. D., *A Novel Approach to Functionalized Nanoparticles: Self-Crosslinking of Macromolecules in Ultradilute Solution,* Advanced Materials, **2001**, *13***,** 204-208.
87. Mecerreyes, D., Huang, E., Magbitang, T., Volksen, W., Hawker, C. J., Lee, V. Y., Miller, R. D. and Hedrick, J. L., *Application of Hyperbranched Block Copolymers as Templates for the Generation of Nanoporous Organosilicates,* High Performance Polymers, **2001**, *13***,** S11-S19.
88. de Moel, K., Alberda van Ekenstein, G. O. R., Nijland, H., Polushkin, E., ten Brinke, G., Mäki-Ontto, R. and Ikkala, O., *Polymeric Nanofibers Prepared from Self-Organized Supramolecules,* accepted in Chemistry of Materials, **2001**.

Abstracts of publications I-VI

I. It is demonstrated that polymeric supramolecular nanostructures with several length scales allow straightforward tailoring of hierarchical order-disorder and order-order transitions and the concurrent switching of functional properties. Poly(4-vinyl pyridine) (P4VP) is stoichiometrically protonated using methane sulphonic acid (MSA) to form P4VP(MSA)$_{1.0}$ which is then hydrogen bonded to pentadecylphenol. Microphase separation, re-entrant closed-loop macrophase separation, and high temperature macrophase separation are observed. When methane sulphonic acid and pentadecylphenol are complexed to the P4VP block of a microphase separated diblock copolymer poly[styrene-*block*-(4-vinyl pyridine)], self-organized structures-in-structures are obtained whose hierarchical phase transitions can be controlled systematically. This microstructural control on multiple length scales (resp. 40 and 350 Å) is then used to introduce temperature dependent transitions in electrical conductivity.

II. Supramolecular hierarchical conducting nanostructures are obtained by complexing amphiphilic oligomers with block copolymers. Nominally each pyridine group of poly(styrene)-*block*-poly(4-vinyl pyridine), i.e. (PS-*block*-P4VP), is first protonated by methane sulphonic acid (MSA) to yield PS-*block*-P4VP(MSA)$_{1.0}$. It is further hydrogen bonded with stoichiometric amount of pentadecyl phenol (PDP) to form PS-*block*-P4VP(MSA)$_{1.0}$(PDP)$_{1.0}$. The polyelectrolytic domains are subject to reversible phase transitions from ”semi 1d” slabs to 2d lamellae and further to 1d cylinders upon heating. The transitions manifest in the thermally activated conductivity. Extension to conjugated polymers is discussed to achieve temperature controlled switching based on electronic conductivity

III. Macroscopic orientation of self-organized supramolecular polymeric materials has been demonstrated by oscillatory shear flow using *in-situ* small angle X-ray scattering (SAXS). In the case when a homopolymer poly(4-vinylpyridine) and pentadecylphenol are stochiometrically complexed to form a comb copolymer-like complex, the self-organized lamellar local structures align parallel when sheared below the order-disorder transition temperature at 60 ^{o}C using 1 Hz frequency and 100 % strain amplitude. Therefore the hydrogen bonds between the phenolic and pyridine groups are strong enough to withstand the applied flow. In the case of a diblock copolymer of polystyrene and poly(4-vinylpyridine) stoichiometrically complexed with pentadecylphenol, the self-organization yields lamellar-*within*-lamellar local structure near room temperature. The larger lamellar diblock copolymer structure showed a parallel orientation upon shearing at 125 ^{o}C (i.e. above the order-disorder transition of the short length scale comb copolymer-like structure) with 0.5 Hz and 50 % strain amplitude. On cooling the short length scale lamellar structure, consisting of poly(4-vinylpyridine) block and pentadecylphenol, is formed inside the layers of the comb copolymer-like material in perpendicular orientation

IV. In this work we present the rheological phase behavior of comb copolymer like supramolecules P4VP(PDP)$_{1.0}$, obtained by hydrogen bonding between poly(4-vinyl pyridine) and pentadecylphenol, during large amplitude oscillatory shear flow experiments over a broad range of frequencies (0.001Hz – 10Hz). The phase diagram, presenting the macroscopic alignment in T/T_{ODT} vs. ω/ω_c , contains three regions of parallel alignment separated by two regions of perpendicular alignment. For our material the order disorder temperature T_{ODT} = 67°C and ω_c, the frequency above which the distortion of the chain conformation dominates the materials' viscoelasticity, is around 0.1Hz at 61°C. The high frequency region of perpendicular alignment, not present in the case of diblock copolymers like polystyrene-*block*-polyisoprene, is likely due to the comb copolymer architecture. For the first time flipping from a stable transverse alignment via biaxial transverse / perpendicular alignment to a perpendicular alignment as a function of the strain amplitude was found.

V. (First paragraph) Hierarchical polymeric materials i.e. *stucture-within-structure* morphologies have interested people due to their potential as functional materials. In this communication we have constructed an assembly of nanoscale protonically conducting "wires" using hierarchical self-organization of polymeric supramolecules. The supramolecules consist of poly(styrene)-*block*-poly(4-vinyl pyridine), i.e. PS-*block*-P4VP, where the latter block forms stoichiometric acid-base complex with toluene sulphonic acid (TSA) which is, in turn, stoichiometrically hydrogen-bonded with pentadecylphenol (PDP), i.e. PS-*block*-P4VP(TSA)$_{1.0}$(PDP)$_{1.0}$. In an effort to achieve "a monodomain", the local structures are aligned globally by shear flow resulting in conductivity enhancement. Protonic transport is macroscopically tridirectional, being largest along the "wires" both below and above the glass transition. The nanoscale structures thus allow tuning of the protonic conductivity and anisotropy in soft materials where the structures have been globally aligned.

VI. (First paragraph) Self-organization leads to nanoscale polymeric structures based on competing interactions and incorporation of several schemes of self-organization renders hierarchical structures. Previously we have introduced a concept where amphiphilic molecules are physically bonded selectively to one block of a block-copolymer to form specific *receptor-substrate supramolecules* and they self-organize to form structure-*within*-structures. Here we demonstrate that the scheme allows the preparation of mesoporous materials. The starting material is diblock copolymer polystyrene-*block*-poly(4-vinyl pyridine), PS-*block*-P4VP, with a stoichiometric amount of pentadecyl phenol, PDP, hydrogen bonded to the latter block. The block lengths have been selected to render a lamellar-*within*-cylindrical morphology, where the P4VP/PDP-blocks form cylinders within the rigid glassy PS-medium and where the P4VP/PDP-complexes, being of a *comb-like* architecture, self-organize as lamellae within the cylinders. In addition to such a local

order, we accomplish overall orientation by applying an oscillatory shear flow to align the cylinders. The orientation is verified using small angle X-ray scattering (SAXS). Hollow cylinders with P4VP brushes at the interior walls are achieved in a straightforward way by dissolving the PDP molecules away from the cylinders, as shown by SAXS and FTIR. Such "hairy tubes" open possibilities for controllable mesoporous membranes as the conformation of the brushes depends on the solvent. In addition, P4VP further allows chemical modification to tailor the membranes.